2. Long Baseline Severe Weather Risk Assessment

2.1. Method Development

2.1.1. Choice of Dataset: Twentieth Century Reanalysis (20CR)

Development of a multi-dimensional discriminant (MDD) model to assess trends and changes in variance of severe weather across North America requires observational records that possess three key elements: (1) a sufficiently-long record in time in order to detect regime changes; (2) the necessary atmospheric variables to diagnose severe weather environments; and (3) spatial coverage over much or all of North America. For climate studies, there are two general sources for observational data: data from individual stations or sites and retrospective or reanalysis products. While station measurements are often considered "truth" for studies, inherent issues with the data (e.g., sparsity of observations and discontinuities in the records) make them challenging to implement for continental-scale analyses as sought in this study. To tackle these challenges with station records, *reanalysis products* (i.e., long-term global-scale datasets that reproduce historical weather conditions) use observational data (e.g., station records, ship data, satellite data, buoys) in data assimilation schemes to recover three-dimensional snapshots of the atmosphere. These products offer temporal and spatial continuity that facilitates large-scale climate studies. The use of reanalysis products for severe weather diagnosis has precedence in the literature [e.g., *Brooks et al.*, 2003; *Gensini and Ashley*, 2011; *Grünwald and Brooks*, 2011; *Lee*, 2012] and is thus appropriate for our work.

We elect to use a newer reanalysis product for this study: the Twentieth Century Reanalysis (20CR) product [*Compo et al.*, 2011]. This dataset has a horizontal resolution of 2° x 2° longitude/latitude globally, a vertical extent in the atmosphere up to ~16 km above mean sea level, and temporally extends from 1873 – 2012 at 6-hourly resolution. Compared to other well-known reanalysis products (e.g., the NCEP/NCAR [*Kalnay et al.*, 1996] and ERA-Interim [*Dee et al.*, 2011] reanalyses), the 20CR has a relatively simple core assimilation scheme; it recovers historical weather patterns from *two* measured variables: surface pressure and sea surface temperatures. Surface pressure data are obtained from the International Surface Pressure Databank, which houses actual pressure observations from international stations from 1871 – present. Ocean conditions are derived from the Hadley Centre Sea Surface Temperature and Sea Ice dataset [*Rayner et al.*, 2003]. These variables are run through an Ensemble Kalman Filter data assimilation system [*Whitaker and Hamill*, 2002; *Whitaker et al.*, 2004] to generate 3-dimensional snapshots of global weather patterns from 1873-2012 (1871 and 1872 are generally ignored as the model needs time to adjust or 'spin-up' to a steady computational state). Another unique facet of the 20CR relative to the other reanalysis products listed is that several realizations of the reanalysis product (i.e., *ensemble members*) can be produced, mainly because only two variables drive its production. Performing these multiple runs with slight tweaks in the input data provides a quantification of the sensitivity of the output fields to potential errors in the input datasets. The resulting atmospheric output variables produced is the *mean* (termed *ensemble-mean*) of those multiple runs, which by construction retains more signal than noise in the output fields.

Compo et al. [2011] offers several exhibits of validation of the 20CR as compared to actual observations (station and radiosonde data) and other reanalysis products. These comparisons offer confidence that this reanalysis product is sufficiently good for use in this study. Furthermore, the 20CR has gained traction in the climate community in several published studies on topics such as long-term oceanic cycles in the Atlantic [*Moore et al.*, 2013; *Alexander et al.*, 2014], trend detection in wintertime storm tracks and the jet stream across the Northern Hemisphere [*Gan and Wu*, 2013; *Woolings et al.*, 2014], and better understanding of El Niño variability [*Anderson et al.*, 2012; *Capotondi*, 2013]. However, like

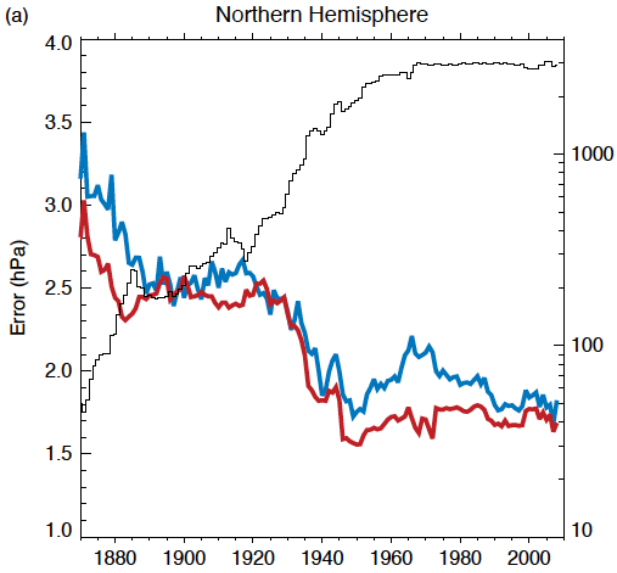

FIG. 2.1 The expected (red) and actual (blue) root-mean-square errors in Northern Hemisphere surface pressure (hPa) between available observations and the reanalysis dataset as a function of year. Thin black line represents the number of observations used in creating the reanalysis data for that year (log-scale on the right). Adapted from *Compo et al.* [2011].

other reanalysis products, changes in data quality and availability through history can impact the output variables and thus possibly generate spurious changes and results. The simplicity of the 20CR, however, reduces the avenues to search for these changes – i.e., changes in the number of surface pressure stations will govern performance metrics for the dataset. **Figure 2.1** (adapted from *Compo et al.* [2011]) illustrates this performance of the model (blue and red curves) change as a function of the number of observations (thin black line) incorporated into the model. From 1870 – 1915, the observational sites increased slowly (note the log scale) and hit a relative minimum just after 1920. Thereafter, the number of observations rose dramatically from ~200 in the early 1920s to nearly 3000 sites in 1960. The response in the root-mean-square (rms) error in the pressure field is a drop of about one-third in expected error (red curve in **Fig. 2.1**) from the early 1920s to the late 1940s with fewer fluctuations in rms error thereafter. Given the change in the observational network and the resulting change in rms error, we have decided to conduct our study from 1940 onwards.

2.1.2. Model Variables

Three primary ingredients favor the formation of severe thunderstorms:

(a) A warm, moist air mass at low and mid-levels of the troposphere, which is inherently unstable and forms convective clouds;

(b) A 'lifting mechanism', which acts as a forcing on the warm, unstable air mass to promote vertical motion and convective cloud development; and

(c) Changes in wind speed and direction with height (termed *vertical wind shear*), which rotates the air column (important for tornado development) and tilts the vertical storm structure that allows a storm to strengthen and develop more vigorous updrafts (important for hail development).

We choose four main variables from the 20CR dataset that encapsulate these primary ingredients and thus represent fundamental atmospheric dynamics associated with severe weather environments. The variables are:

(a) **Convective Available Potential Energy** – Convective available potential energy (CAPE) represents the amount of energy that air parcels gain as they are vertically lifted from the bottom of a cloud through the free troposphere. Large values of CAPE indicate a strong propensity for vigorous convection to develop, while small or no CAPE is prohibitive for severe weather development.

(b) **2-4 km Lapse Rate** – Temperatures in the troposphere generally decrease as one goes higher within the layer. The lapse rate measures this change, in this case between 2-4 km

above ground level (AGL): i.e., $Lapse\ Rate = -\frac{T_{4\ km} - T_{2\ km}}{2\ km}$, where T is temperature and the negative sign is used for meteorological convention (i.e., a decrease in temperature with height is a positive quantity). Air masses with large lapse rates (typically > 6.5°C/km) are inherently unstable and can support severe weather environments.

(c) **Low-Level Divergence (DIV)** – We use horizontal mass divergence/convergence of air in the lower 1.5 km of the atmosphere as a measure of a lifting mechanism for severe weather. Converging (DIV < 0) air in the low-levels of the atmosphere can only rise in order to maintain mass conservation. This rising air can cool and condense to form clouds and precipitation. If this forced rising motion occurs in highly unstable, high CAPE regions, these clouds can then grow to form vigorous convection and possibly severe weather.

(d) **0-6 km (AGL) Speed Shear –** Termed *bulk shear* in meteorology, this quantity measures the change in speed of the winds between the surface and roughly the middle troposphere. As mentioned, high shear environments produce strongly favorable severe weather environments.

Selection of these first-order physical variables roots our subsequent work in actual dynamics of the atmosphere and not on, for example, empirically-derived indices. Thus, the relationships derived by our MDD are more impervious to statistical non-stationarity concerns. For all variables, we use the 1800 UTC daily value (i.e., 2:00 PM EDT) for the MDD, which is close to the time of maximum heating and hence the most instability for much of North America (except the West Coast, where severe weather occurrence is small anyways). Analysis was also done with other times available from the 20CR dataset (0000, 0600, and 1200 UTC), and 1800 UTC produced the best correspondence with the SPC spotter reports used for model training.

Guidance in the choice of these variables is rooted in both operational meteorology (i.e., variables that forecasters used to predict severe weather events) along with established literature on severe weather trends and diagnosis. For example, *Brooks et al.* [2003] performed a linear discriminant analysis using convective CAPE and shear to diagnose significant severe weather environments over a 3-year period from NCEP/NCAR reanalysis. In addition, the study considered the lapse rate of the environment as an additional discriminator for event selection. *Gensini and Ashley* [2011] constructed an empirical index comprised of a variant of CAPE (MUCAPE) and bulk shear to study trends in severe weather across the US over the latter half of the twentieth century. The CAPE-shear framework for severe weather environment is also used to assess the impacts of severe weather environment frequency through the twenty-first century under future climate change [e.g., *Marsh et al.,* 2007, 2009; *Trapp et al.*, 2007, 2009; *van Klooster and Roebber*, 2009; *Brooks,* 2013].

The CAPE-shear framework does not capture the key 'lifting mechanism' ingredient needed for severe weather, however. Recognizing this shortcoming, we explicitly added DIV as a first-order variable into our MDD model. Studies like *Lee* [2012] and *Lock and Houston* [2014] explicitly added DIV or similar variables (i.e., changes in low-level geopotential height fields) to detect a forcing mechanism for severe weather environments. We adopt this extra variable to add more dynamic and physicality to our discriminant analysis.

One additional variable is computed and used for diagnosing our severe weather environments: the freezing level of the atmosphere (i.e., the height AGL at which the temperature first reaches 0°C). This variable is especially important for hail formation, as this metric designates the thickness of the melt

layer into which hail must pass before reaching the ground. More about the use of the freezing level in the MDD is discussed in **Section 2.1.5.**

2.1.3. Model Method

We developed a model to identify environments favorable for perilous weather (hail/tornado/wind) using the four variables described in the previous section and spotter records from the NOAA Storm Prediction Center (SPC) Severe Weather Database[1]. These records represent reports compiled by local National Weather Service offices from trained spotters, official reports, and news reports. Although the historical spotter records of severe weather events date back to the 1950s, we restrict the records used for model development to the 1999-2012 period to avoid large biases in the database due to changes in reporting standards/procedures/frequency as well as population growth/expansion. We focus on three perils in particular: hail, tornado, and wind. Because peril depends differently on our model four variables (**Section 2.1.2**), we train each peril independently against the SPC reports. Although we choose to utilize only the most recent decade of storm reports to avoid large observational biases, we still expect the 1999-2012 SPC spotter reports to favor events that occur near locations with higher population or valuable assets. The biases, however, appear to be small in general and do not appear in long-term climatologies of our results (see **Section 2.2.4**).

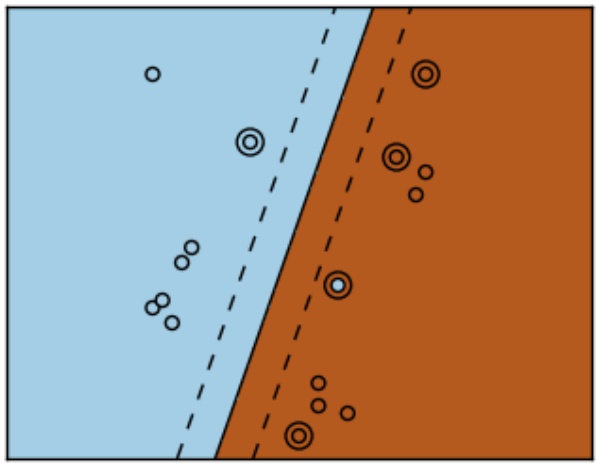

FIG. 2.2. Example of a discriminating plane formulated by SVM maximizing the distance between points of each class (blue, brown) and the plane.

The multi-dimensional discriminant (MDD) model utilizes the linear support vector machine (SVM, *Cortes & Vapnik 1995*) algorithm. The SVM algorithm creates a hyperplane containing the input environmental variables and peril classification. To ensure that the four input environmental variables are on the same scale, we mean-normalize each of the variables to the 20-year mean/min/max values at that grid location for that day of year. At each grid location on each day in the training period, we label the four variable values with a classification of "1" if a severe weather event has occurred on that day within the grid box, and a "-1" otherwise. The SVM model then formulates a discriminating plane that separates the two classes for all days at all locations in the training set. The discriminating hyperplane is optimized by maximizing the distance between points belonging to each of the two classes. **Figure 2.2** illustrates the optimization of a dividing hyperplane by the SVM algorithm in a simple, two-dimensional case.

We choose a linear implementation of SVM for its simplicity for physical interpretation – the resulting dividing plane is simply a vector of four values that can be interpreted as the relative importance, or weights, of each variable to the classification of whether the environment may/may not produce severe weather events. Because we choose a simple linear implementation of SVM, there will inevitably be misclassifications as points end up on the wrong side of the plane (i.e. – blue dot in the brown plane in **Figure 2.2**). The vector can then be used to identify severe weather environments at different locations and times in the rest of the 20CR dataset. More complicated, non-linear kernels are available for the

[1] www.spc.noaa.gov/wcm/#data

SVM method, but they do not allow for straightforward physical interpretations and, more importantly, do not appear to perform much better than the linear implementation.

To ensure that the discriminating plane is not strongly dependent on the choice of input dataset, we trained randomly selected subsamples (50% of the entire training set from 1999-2012) and tested the discrimination algorithm on the other half of the training set multiple times. We discuss the stability of the model in **Section 2.2.1**. We note here that the MDD model we have developed using the SVM method does not make any claims about the *severity* of the hail/tornado/wind event that may be associated with the weather conditions (i.e., a F1 vs. a F5 tornado), but rather identify *environments* that are favorable for perilous weather events. Additionally, the severe weather environments do not necessarily imply a severe weather event – there is some efficiency in which the environments result in observed events, which we quantify in **Section 2.2.3**.

2.1.4. Region Description

The four main variables we use in the MDD represent the physical fundamental dynamics behind convective formation. As stated in the MDD description, these variables are mean-normalized at the grid-point level. The spatial scale for the SVM framework for derivation of the weighting factors can be done at any spatial scale. At one extreme, the SVM could be trained across the contiguous United States. The problem with this approach is that normalized values of a variable can have widely different values depending on the location and hence have very different physical interactions. For example, a normalized value of 0.5 in CAPE could represent 3000 J/kg of CAPE in a region with climatologically-high CAPE (e.g., the Front Range of the Rockies) or 300 J/kg in the Pacific Northwest. These two actual values of CAPE offer very different energetics for the atmosphere to support or not support convection. At the other extreme, the SVM could be trained at each and every grid point across North America. Aside for the tremendous computational expense, the problem with this approach is that the actual verified events in that grid cell required for training the MDD would be far too few to produce meaningful, consistent weights for analysis.

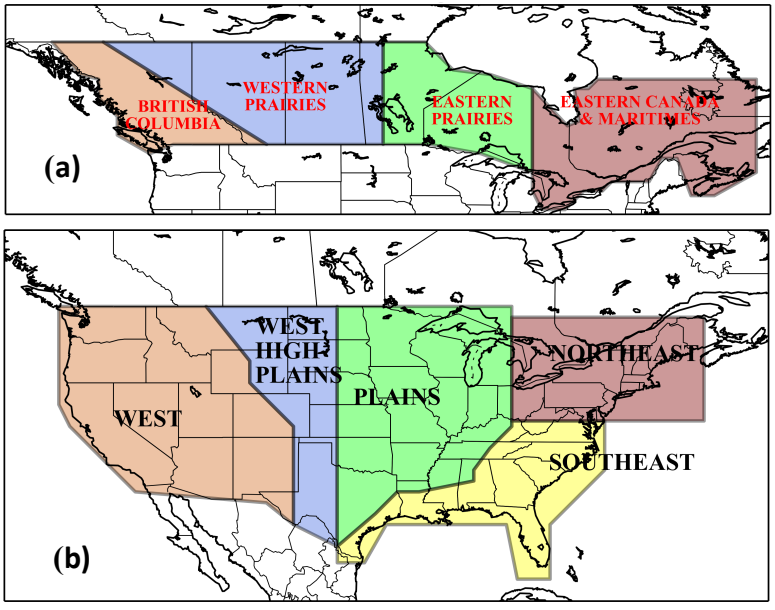

FIG. 2.3. The regions chosen for MDD training and evaluation for (a) Canada and (b) the United States.

Hence, we adopted a *regional MDD analysis* to try to balance the disadvantages of the two extremes described above. **Figure 2.3** presents a map of the regions used in our study for MDD modeling for both Canada (**Fig. 2.3a**) and the United States (**Fig. 2.3b**). These regions were chosen based on three main criteria: (1) major geographical features (e.g., the Rocky Mountains and the Gulf of Mexico), (2) meteorological and climatological knowledge of thunderstorm parameters in different areas (e.g., the Southeast experiences high CAPE/low shear environments for thunderstorms, while the Western High Plains are regions of very high CAPE and lapse rates in contrast to other regions); and (3) the climatological distribution of severe weather (e.g., the

British Columbia/West regions experience few incidents of severe weather, whereas the Plains and Western Prairies experience high incidents of severe weather). Support for regionalization in determining severe weather environments and their characteristics exists in other similar studies [e.g., *Brooks et al.*, 2003; *Grünwald and Brooks*, 2011; *Gensini and* Ashley, 2011; *Robinson et al.*, 2013].

Note that model training/development utilizes only data in the 1999-2012 period from the US where SPC spotter reports are available, and the resulting weights are used in the corresponding regions in Canada (**Figure 2.3a**) and the US for the entire 1940-2012 period.

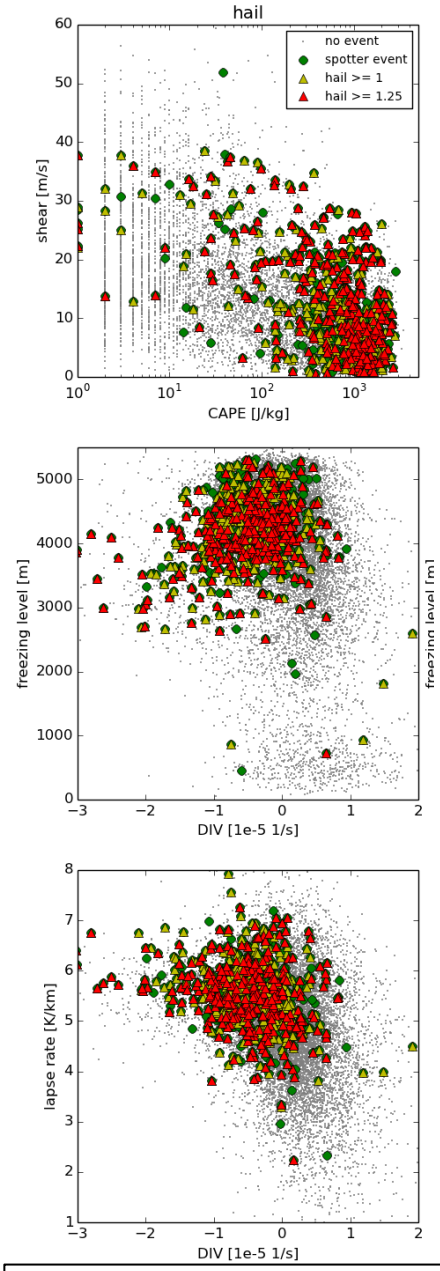

FIG. 2.4. Example of how the limits for the threshold filtering are chosen for severe hail environments in the Southeast.

2.1.5. Physically Based Threshold Filtering

To improve the performance of the MDD model, environments pre-classified as unlikely to produce severe weather are excluded from the training and discrimination process using some simple thresholds (CAPE > 0, DIV < 0, shear > 0, lapse rate > 0). After training the model, we impose a second filter with stricter regional limits on the environments for the discrimination process. As shown in **Figure 2.4**, the second filter requires the severe weather environments to be within some parameter space where most of the intense hail/tornado/wind SPC reports reside.

This second pass through the discrimination results increases the performance of the model against verified events by reducing the number of unverified events (i.e. - events classified as severe weather environments, but do not have corresponding SPC reports in our testing runs). At this point in the modeling process, we include the fifth variable from the 20RC, the freezing level, in the filter. The freezing level indicates the above ground level where the temperature is at freezing. If the freezing level is too low, then the lower atmosphere is too cold to support severe weather environments. If the freezing level is too high, then the melt layer below it will be too thick for hail to survive to the ground.

We chose to include an additional variable and impose the stricter limits post- instead of pre-classification due to the nature of our discrimination algorithm. Given the linear nature of our model, including the freezing level in the SVM model would introduce too many degrees of freedom to improve the algorithm. Additionally, imposing the stricter limits would exclude too many points for stable model development.

Figure 2.4 shows an example of how the limits for hail in the Southeast region of the US are derived from scatter plots of environmental variables for each day at each grid point, with SPC spotter reports of hail at different levels shown with different symbols. Based on the distribution of the red and yellow triangles in the various parameter spaces, we require hail environments identified by the MDD algorithm to have CAPE > 100 J/kg, DIV < 0, 0 < shear < 50 m/s, lapse rate > 4

K/km, and 2000 < freezing level < 5000 m.

2.2. Model Validation

2.2.1 US Model Stationarity

We test the stability of the discriminating plane created through the SVM method by randomly selecting half of the points from the 1999-2012 dataset for training and the scoring on the remaining half. We find that the weighting factors (used to form the discriminating plane to classify severe versus non-severe weather environments) typically vary by < 10% from the mean for all the runs. In cases where the weighting factors that deviate from the mean by > 10%, the weighting factor is often close to zero, implying that the variable does not correlate well with the observed peril.

2.2.2. Model of US Catastrophes

We consider the performance of the MDD model by mapping the severe weather environments for catastrophic historical weather events compiled by Property Claims Services (PCS). PCS defines catastrophes as events that cause $25 million or more in direct insured losses in the United States.

The left panels of **Figures 2.5, 2.6, and 2.7** show examples of hail, tornado, and wind environments on days of catastrophe events recorded by PCS, with the event date and PCS event number noted in the title. The right panel of **Figures 2.5 and 2.7** shows the corresponding report from the SPC Severe Weather Database aggregated to the same grid resolution as the 20CR. For the 1974 super tornado outbreak, one of the worst in US history with 148 tornadoes touching down in 24 hours, we show map of the actual tornado tracks in **Figure 2.6b** to illustrate the extent of the tornado outbreak.

In all three cases, the MDD model did a good job identifying severe weather environments that may lead to hail, tornado, or wind events, as shown in the maps of reported events. In most cases, however, the model also identifies environments that do not have corresponding reports of severe weather: either the actual event was not observed/reported (bias against areas of low population), or the severe weather environment did not lead to an event. We can consider the latter case as an *efficiency factor* for translation from severe weather environments to events, which we quantify in **Section 2.2.3**.

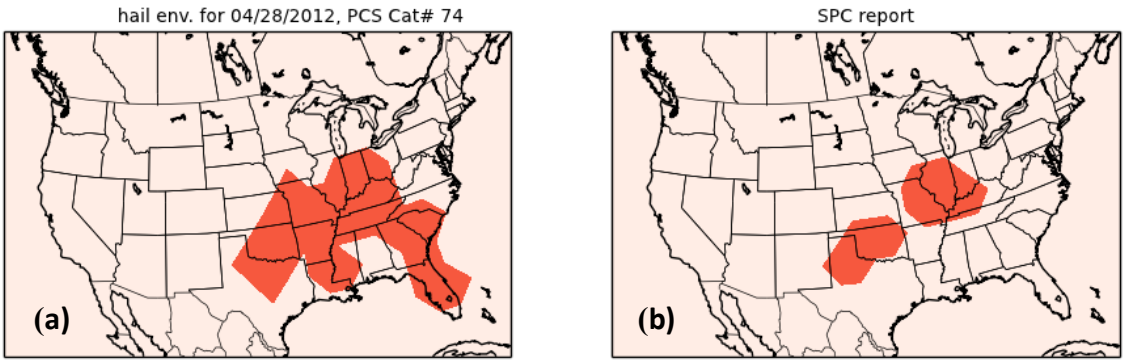

FIG. 2.5. (a) Hail environments for PCS Cat event #74 on April 28th, 2012, that affected Illinois, Indiana, Kentucky, Missouri, and Texas. (b)The Storm Prediction Center hail reports for the same day.

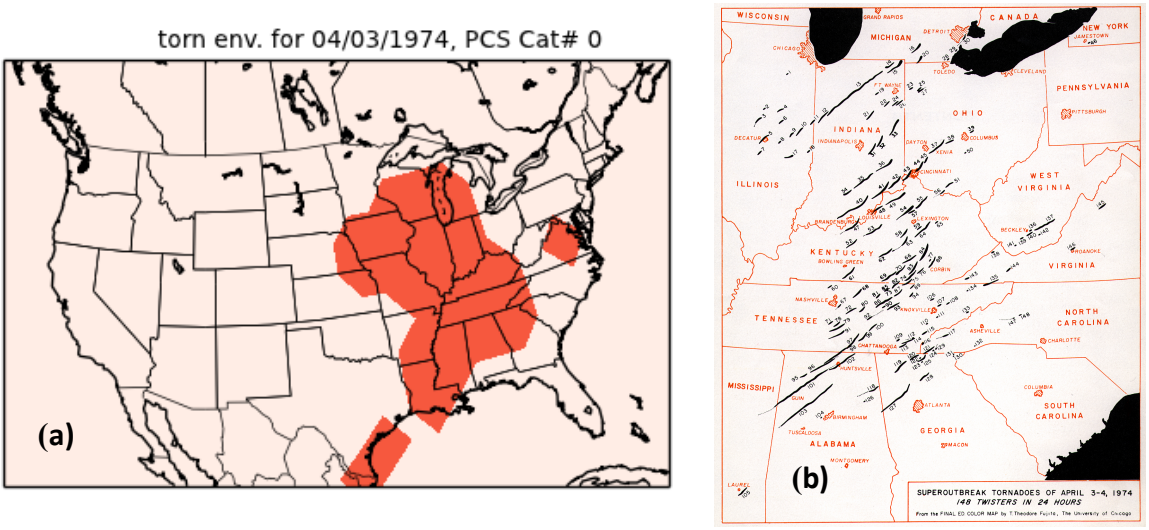

FIG. 2.6. (a) Tornado environments for one of the largest tornado outbreaks in the history of the US, which 148 tornadoes touching down in 13 states between April 3rd and 4th of 1974. (b) Map of tracks for all tornadoes from the outbreak [*Fujita 1975*].

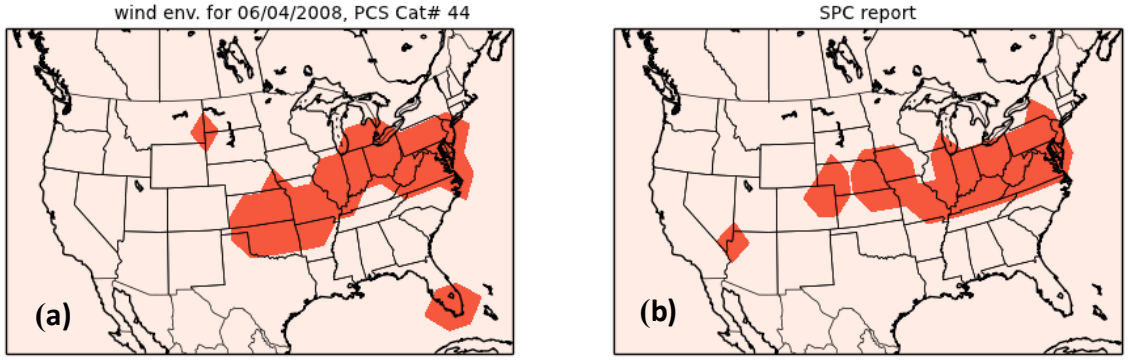

FIG. 2.7. (a) Wind environments for PCS Cat event #44 on June 4th, 2008, that affected Iowa, Illinois, Indiana, Kansas, Maryland, Missouri, Nebraska, Oklahoma, Virginia, and West Virginia. (b) The Storm Prediction Center wind reports for the same day.

2.2.3. Spatial Distribution of Efficiency Estimates

As discussed in **Section 2.1.3**, there appears to be some efficiency factor that translates the severe weather environments we identify to observed severe weather events. We again utilize the 1999-2012 hail, tornado, and wind reports from the SPC Severe Weather Database to estimate this factor at each grid location. For each peril, we take the ratio of the total number of SPC-observed events to the number of severe weather environments identified over the 14-year period at each grid location. To avoid population biases that lead to an increase in reports near population centers, we spatially smooth the spatial distribution of the efficiency factors with a 2-dimensional Gaussian function.

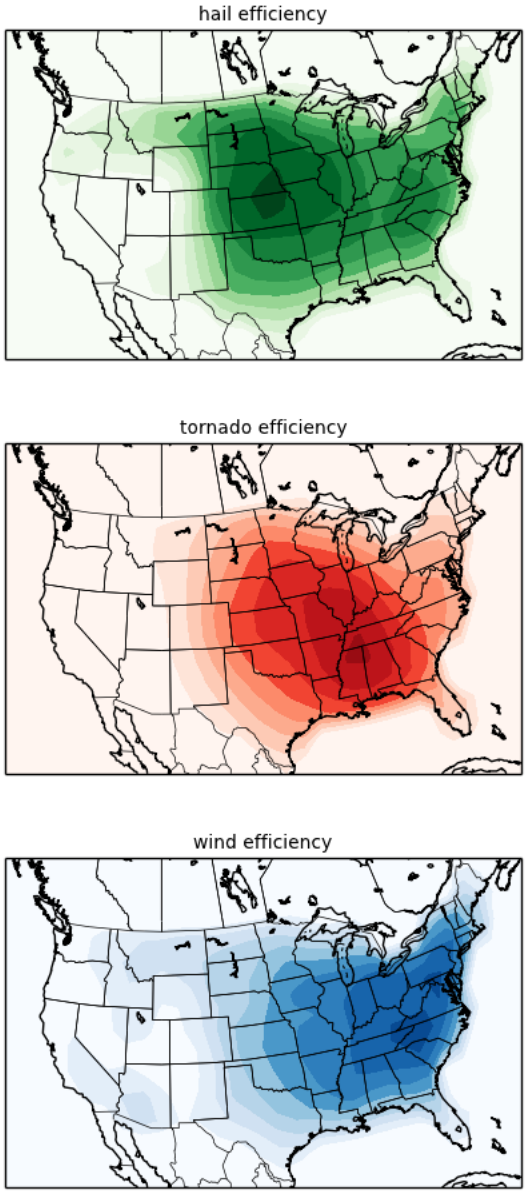

FIG. 2.8. Spatial distribution of the efficiency factors relating severe hail/tornado/wind environments identified by the MDD model to observed reports of hail/tornado/wind from the SPC.

Figure 2.8 shows the smoothed spatial distribution of the efficiency factor for each peril, where darker colors reflect higher efficiencies. Excluding the West, where the efficiencies are very low (~5% for hail and wind, ~1% for tornado), the average efficiency for the US is ~20% for hail and wind, and ~5% for tornado. The lower performance of the MDD model in the West is primarily due to the lack of hail and tornado events to train against. When analyzing the results from the MDD model for the US, we can then apply the spatially dependent efficiency factors to estimate the number of events that may have occurred in a given year at a specific location.

We find that, for cumulative plots that sum over regions or the entire country (**Sections 3.1.1, 3.1.2**), applying the efficiency factors simply scale the results down and do not change the trends that we observe. Thus to facilitate a straightforward comparison with Canadian results (where we cannot calculate efficiency factors due to the lack of uniform hail/tornado/wind reports) when possible, we only apply the efficiency factors when we consider the spatial distribution of severe weather environments.

2.2.4. US Climatology 1940-2012

After applying the spatial efficiency factors to our results, we consider the long-term climatology of the different severe weather environments. **Figure 2.9** shows the total hail/tornado/wind environments for the United States, summed over the 1940-2013 period of analysis. The spatial distribution of the severe weather environments appears reasonable – the incidence of severe weather environments for all perils is very low west of the Rocky Mountains, and peaking in the Plains and Southern regions as expected.

Figure 2.9a shows hail environments peaking in the Central Plains in Kansas, where severe hail often occurs,

although a secondary peak along the Southern Atlantic Coast is interesting. The distribution of tornadic weather environments is also reasonable – tornado alley (Texas, Oklahoma, Kansas, Nebraska) appears high in **Figure 2.9b**, although the peak is centered further to the east. The long-term climatology of severe wind environments is curious – we expect large convective winds to be centered along the Central Plains, but instead it peaks along the Southern Atlantic Coast.

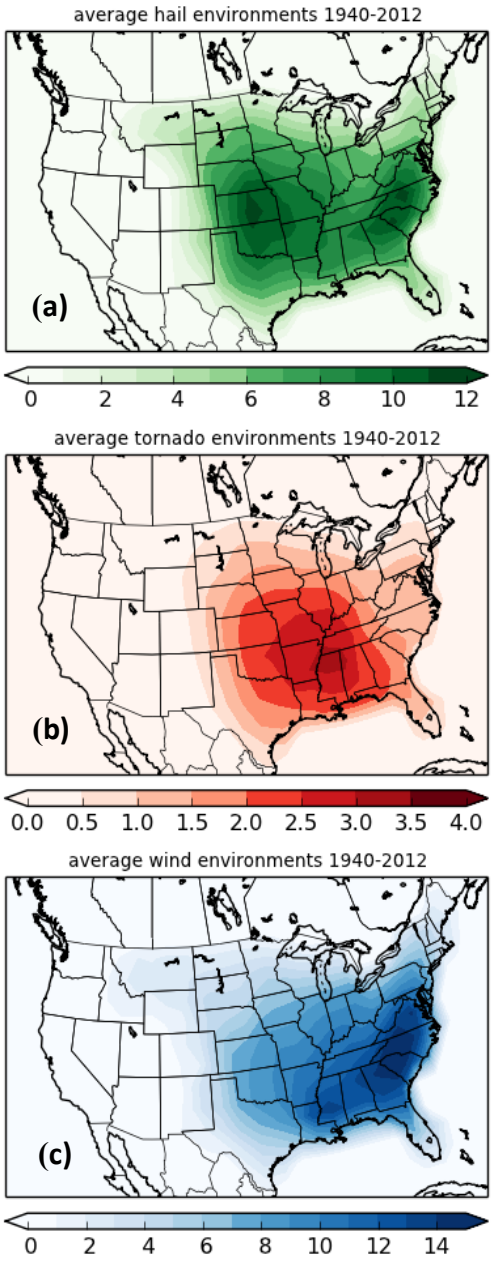

FIG. 2.9. Climatology of (a) hail, (b) tornado, and (c) wind environments for the 1940-2012 period.

To better understand the climatologies of the severe weather environments we identified with the MDD model, we compare our results with published climatologies for hail, tornado, and wind. **Figure 2.10b** shows the probability for hail > 2.0" for the 1995-1999 period *from Doswell et al. [2005]*. As mentioned previously, the peak observed in the Central Plains by the MDD model (**Figure 2.10a**) is expected, and well matched to the area of highest hail probability. While the secondary peak along the Southern Atlantic Coast does not appear in Doswell's climatology for hail > 2.0", it is well-matched to **Figure 2.10c**, where *Doswell et al. [2005]* show the daily probability for all hail > 0.75". This suggests that the MDD model does an excellent job in identifying environments that may result in large as well as more moderately-sized hailstorms.

Figure 2.11 compares the 2003-2011 climatology for tornadic environments against the kernel density estimate of convective tornados for the same period from *Smith et al. [2012]*. Overall, there is good correspondence between the peaks of both climatology distributions, centered on Arkansas/Mississippi. The shape of our climatology distribution at lower contour levels, however, does not match the Smith distribution as well, most likely due to the lower accuracy/efficiency of our model.

Finally, we compare the climatology for severe wind environments from our model against kernel-density smoothed climatology for convective wind reports from *Doswell et al. [2005]* in **Figure 2.12**. Of the three perils we model, the severe wind environment climatology appears to be the least well-matched to published climatologies. Instead of the three peaks observed in the Doswell climatology, our model shows one large, smooth peak along the East Coast. This is likely due to the coarse 2° degree grid of the 20th century reanalysis dataset we use to identify severe weather environments, which could serve to smooth out features on smaller spatial scales. Additionally, the third peak near the Central Plains do not appear as strongly in our model – this is perhaps due to population/observational biases that favor the East Coast in the wind spotter data we train our model against. The overall distribution of the two climatologies, however, appears reasonably similar.

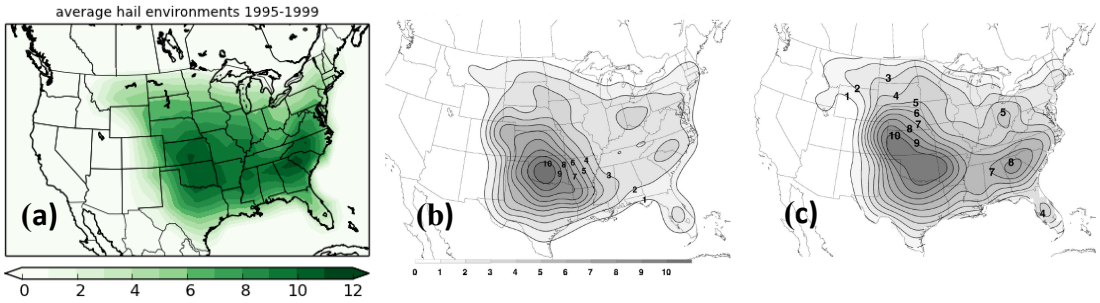

FIG. 2.10. (a) Climatology for hail environments for the 1995-1999 period identified by our MDD model. (b), (c) Smoothed probability of hail > 2.0" and 0.75", respectively, for the period 1995-1999 *[Doswell et al., 2005]*.

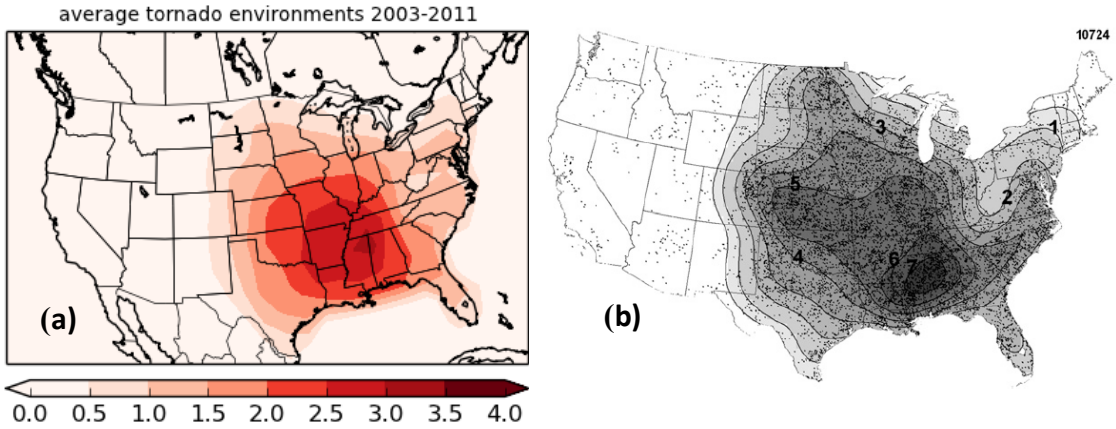

FIG. 2.11. (a) Climatology for tornado environments for the 2003-2011 period identified by our MDD model. (b) Contours of the kernel density estimate of convective tornado events for the same period, starting at 1 event every 10 years, dots represent actual tornado reports *[Smith et al., 2012].*

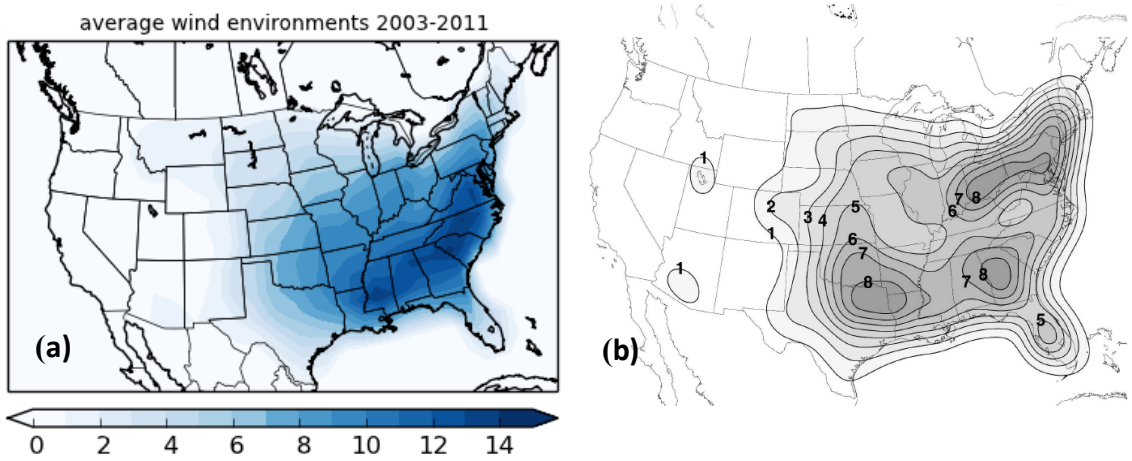

FIG. 2.12. (a) Climatology for severe wind environments for the 1995-1999 period identified by our MDD model. (b) Smoothed probability of convective wind events for the same period *[Doswell et al., 2005]*.

2.2.5. Model of Canadian Catastrophes

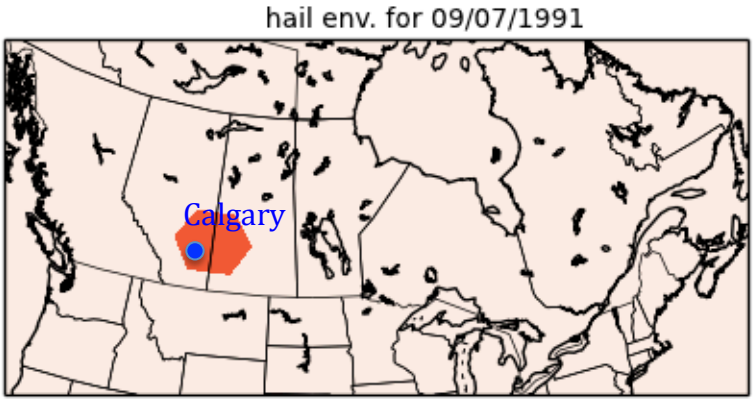

FIG. 2.13. Hail environment over Calgary, Alberta on September 8th, 1991, that is associated with a hailstorm resulting in $342 million CAD in damage.

We consider how well the MDD model translates to Canadian regions by mapping the severe weather environments for catastrophic historical weather events. We select one of each peril from the ten most costly losses in Canada from 1983-2013 *[Insurance Bureau of Canada, 2014]*. Because we do not have analogous SPC reports for Canada for comparison, we note the location affected by each event on the maps.

The 1991 hailstorm in Calgary is one of the most costly in Canadian history. Only 30 minutes in duration, the storm resulted in $342 million CAD in damage ($508 million in 2013 dollars). The MDD model accurately identified the grid cell containing Calgary, Alberta as a hail environment for the day of the storm (**Figure 2.13**). In 2012, a severe weather system traveled eastward across Canada from Thunder Bay, Ontario, to Montreal, Quebec in May, driving a slew of wind/thunderstorms that resulted in $260 million CAD in damage. **Figure 2.14** shows how the model identified the wind environments in these areas as the front traveled from west to east.

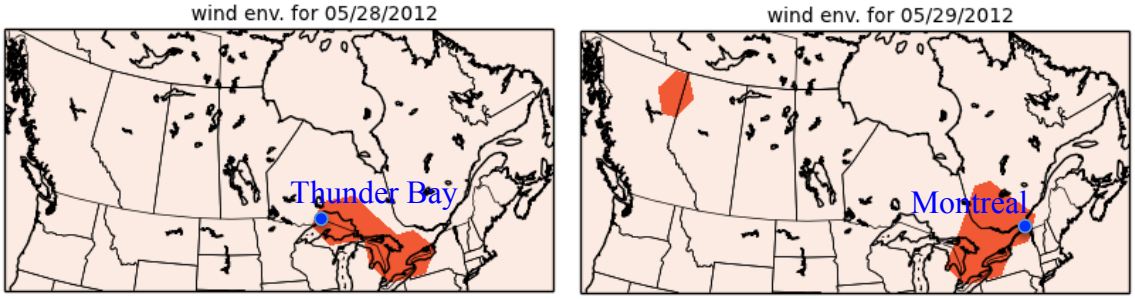

FIG. 2.14. Wind environments over Thunder Bay, Ontario and Montreal, Quebec associated with a multi-day storm in May of 2012, resulting in $260 million CAD in damage.

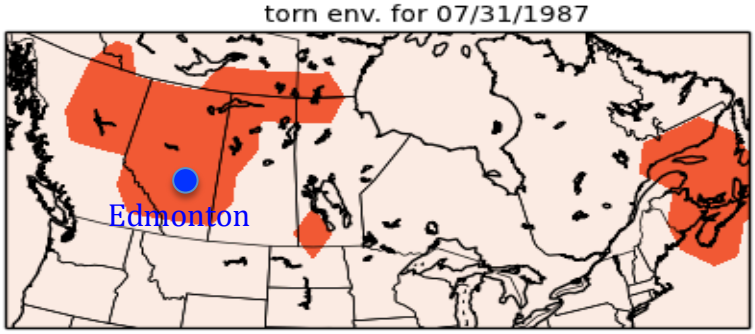

FIG. 2.15. Tornado environments over Edmonton, Alberta on July 31th, 1987, associated the "Black Friday" tornado, resulting in $148 million CAD in damage.

On July 31, 1987, a F4 tornado tore through Edmonton, Alberta, causing $148 million CAD in damage ($266 million in 2013 dollars) along a 40 km path of destruction. **Figure 2.15** shows that the model correctly identified the region around Edmonton as a severe tornado environment. However, it also identified other regions as severe tornado environments where there

were no tornado reports on that day. This is again related to the efficiency of severe weather environments resulting in actual events. Because we do not have a set of peril reports analogous to the SPC reports in Canada to calibrate against, we do not estimate efficiency factors for the different grid locations as we did for the US in **Section 2.2.3**.

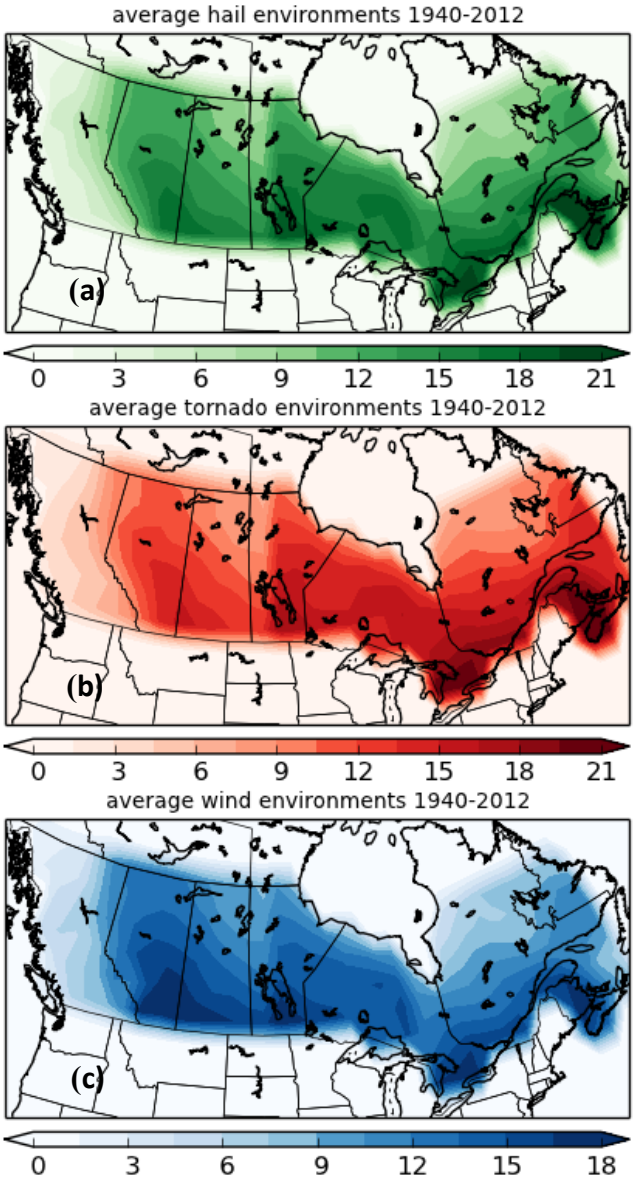

FIG. 2.16. Climatology of (a) hail, (b) tornado, and (c) wind environments for the 1940-2012 period.

2.2.6. CANADIAN CLIMATOLOGY 1940-2012

We also consider the long-term climatology of the different severe weather environments for Canada over the 1940-2013 period (**Figure 2.16**). Note that average number of severe weather environments for the different perils appear to be *higher* because we do not calculate efficiency factors for Canada – there are no standardized reports of hail/tornado/wind over a sufficiently long period of time to calibrate our model against. If we assume that the efficiency factors for US averaged over all grid points (excluding the West) translates into Canada, then we expect the numbers to be scaled down by ~80% for hail/wind, and ~95% for tornado. In any case, since we are most interested in detecting trends in the number of severe weather environments over time, it is the number of environments relative to each other over time that matters.

While the long-term climatologies of the three perils appear similar, there are noticeable differences between the distributions, especially in the shape around Alberta/Saskatchewan. **Figure 2.17** compares the hail climatology from 1951-1980 against the average number of hail days per year over the same time period *[Environment Canada 1987]*. The distribution of hail environments from the MDD model appears to be quite similar to the Environment Canada climatology in the Alberta, Saskatchewan, and lower Manitoba provinces. In fact, if we reduce the number of environments by 80% using the average US efficiency factor, the number of hail days per year in these regions (~2-4) corresponds very well with the Environment Canada numbers (3-5). The one major mismatch is the large number hail environments in Ontario and Eastern Canada in the MDD climatology that do not appear in the Environment Canada climatology.

Figure 2.18, showing the distribution of average lightning flash density annually, may shed some light to this issue. Associated with thunderstorms, we can consider lightning as a proxy for severe weather environments. The high density of lightning flashes near Toronto and along the southern parts of Ontario and Quebec provinces is well matched to the hail climatology from the MDD model. This

suggests that our hail model is accurately identifying severe weather environments, although these environments may not result in hail in the eastern Canadian provinces.

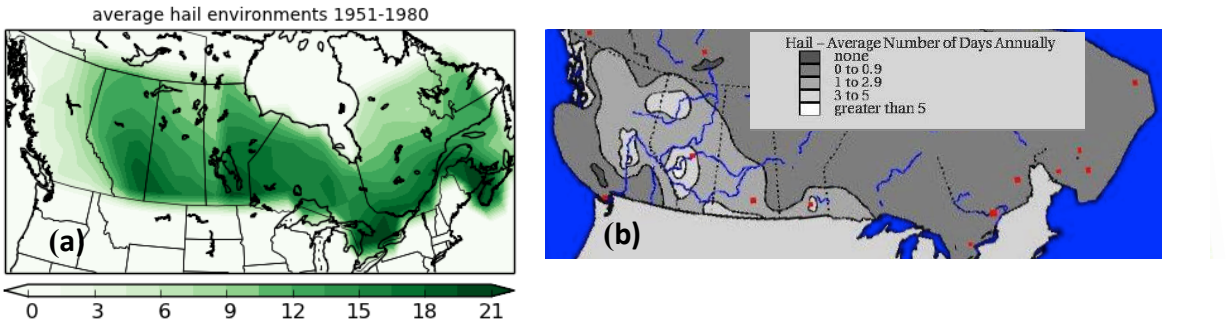

FIG. 2.17. (a) Climatology for hail environments for the 1951-1980 period identified by our MDD model for Canada. (b) Average number of hail days per year for the same period *[Environment Canada, 1987].*

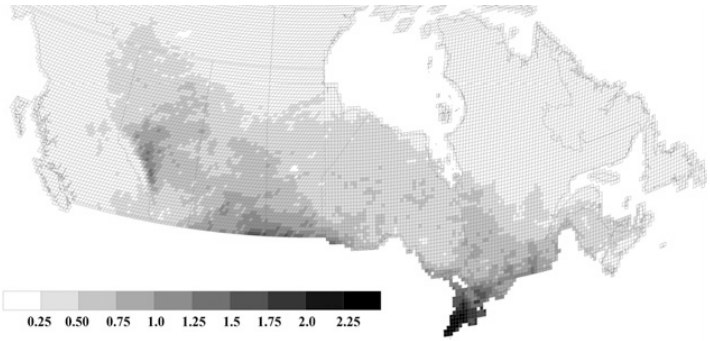

FIG. 2.18. Mean annual lightning flash density (#/km^2/year) for the 1999-2009 period *[Chang et al. 2013]*, which can be considered as a measure of thunderstorm weather environments.

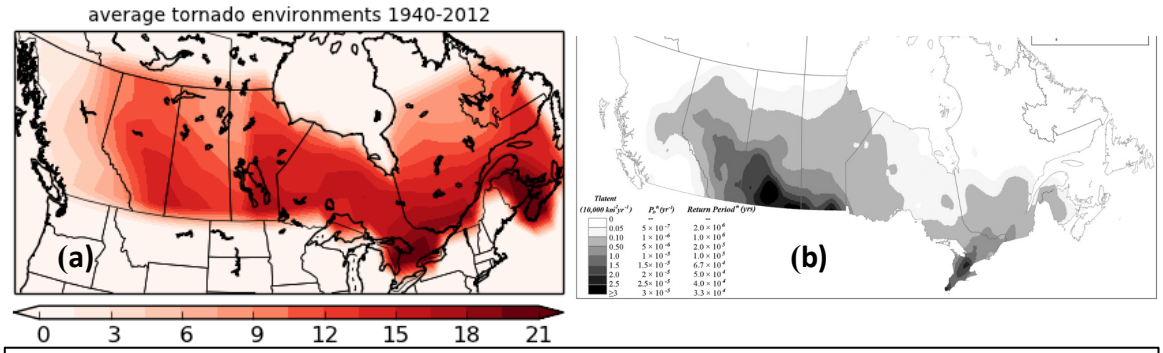

FIG. 2.19. (a) Climatology for tornado environments for the 1940-2012 period identified by our MDD model. (b) Predicted tornado occurrence (#/year for a ~1x1° box) from *Chang et al. [2013].*

Figure 2.19 compares the climatology of tornado environments from the MDD model against the predicted tornado occurrence from *Chang et al. [2013]*. Similar to the hail climatology, our model is well matched to the predicted occurrence in the British Columbia, Alberta, Saskatchewan, and Manitoba provinces. Additionally, the high density region in Toronto and southern Quebec province we observe can also be seen in the predicted tornado occurrence, although southern Ontario and the region around New Brunswick appears to be too high.

Finally, we attempt to compare our severe wind environment climatology against published climatologies, which appears to be sparse. There are no climatologies that cover the entire country, but **Figure 2.20** shows the average number of severe wind events per year between 1982-1991 for Alberta *[Paurk & Blackwell, 1994]* and the total number of severe wind events in Ontario between 1979-2009 *[Environment Canada 2012]*. Even though the periods are slightly different, our wind climatology compares quite well with the average number of wind events per year in Alberta: the locations of the 15-18 events/year contours in our MDD results line up with the *Paurk & Blackwell* contours of 10-20 events/year. For the Ontario Province, both our MDD and the Environment Canada distributions peak around the Toronto region, but the rest of southern Ontario in the MDD model appears to be higher than observed. This is again likely due to the algorithm picking up on severe weather environments associated with lightning (**Figure 2.18**) that may not have produced extreme wind events.

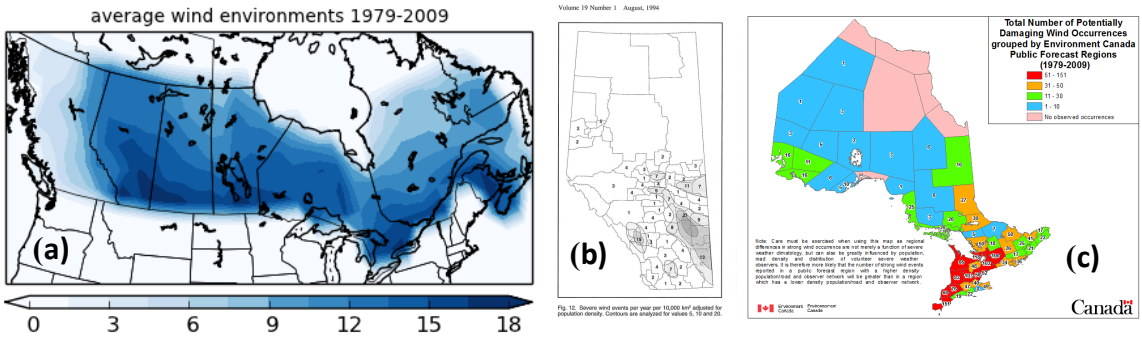

FIG. 2.20. (a) Climatology for wind environments for the 1979-2009 period identified by our MDD model. (b) Averaged severe wind events per year for the period of 1982-1991, with contours of 5, 10, and 20 events/year *[Paurk & Blackwell, 1994]*. (c) Total number of severe wind events in the Ontario Province from 1979-2009 *[Environment Canada 2012].*

3. Long Term Analysis

3.1 US

3.1.1. Overall Trends

We begin our investigation by examining the annual nationally-aggregated number of severe weather environments in the Lower 48 from 1940—2012, delineated by peril (**Figure 3.1**). The 73-year trend in all peril environments is nearly flat, though there is considerable inter-annual variability visible in the environments. Periods of high hail and wind environments (**Fig. 3.1a** and **3.1c**) are seen in the late 1950s and the early-to-mid 1970s. High variability in the 1980s in the hail and wind perils then yielded a slight downward trend in total number from the 1990s into the 2000s but with higher variance. Tornado environments (**Fig. 3.1b**) illustrate some heightened activity visiting in the late 1950s and again somewhat in the early 1970s. Thereafter, the counts remain relatively flat in number and also variance before variability increases again in the post-1998 to present period. Testing for 10, 15, and 20-yr trends, throughout the record, only the downward trend of hail environments from 1991—2010 is significant (trend = -513 hail env./decade; $p < 0.05$ per the Mann-Kendall test). The flattening or slight decline in the hail and wind environments over the US agrees well with *Gensini and Ashley* [2011]. Further examination of agreement in trends is reserved for **Section 4**.

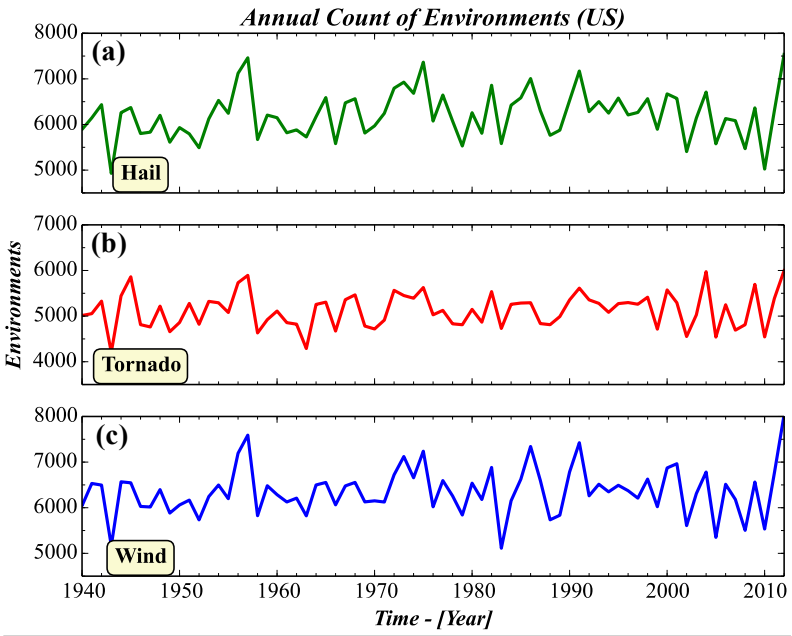

FIG. 3.1. The annual counts of (a) hail, (b) tornado, and (c) wind environments from 1940—2012 across the entire US.

Figure 3.2 displays the same annual environments over the contiguous US but with a 5-year running mean applied to the data, along with a 5-year running standard deviation in the environments (gray shading). The 5-year running means of the annual counts of severe weather environments show more clearly the trends and other statistical properties previously described and evaluated. Focusing on the late 1990s through the 2000s, the envelope of 5-year standard deviations stands between 450-600 severe weather environments for each peril, with the wind peril at the higher end of the deviations. In examining prior 5- and 10-year periods, the 2008—2012 and 2003—2012 standard deviations are significantly different (i.e., higher) than the relatively high variability of the late 1940s-1950s ($p < 0.05$). However, the variance in the twenty-first century is *not* significantly different than the period of high variability seen during the early-mid 1940s and mid-1950s for all perils nor is it significantly different from the high variability of the 1980s for the wind and hail perils (**Figs. 3.2** and **A.X**). Hence, *while the recent 5-10 years have illustrated a degree of high variability in the perils across the US, the variance experienced is not unprecedented according to the MMD analysis*

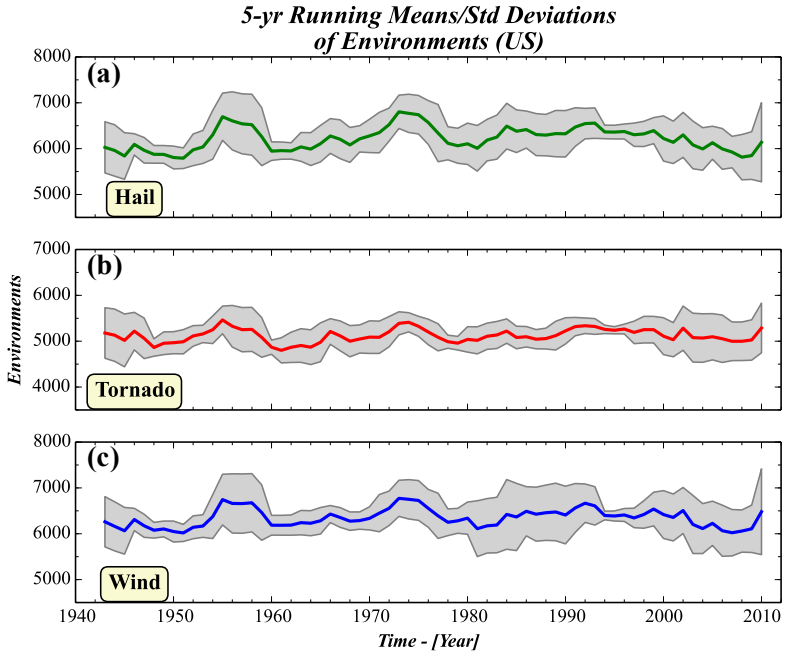

FIG. 3.2. 5-year running means of annual (a) hail, (b) tornado, and (c) wind environments from 1940-2012 across the contiguous US. Gray shading represents ±1 standard deviation (5-year running) of the environments.

We also consider trends in the number of days per year with widespread severe weather environments. Across the contiguous US over our 73-year record period, we find the average number of severe weather environments to be ~16 per day, we choose a threshold of 40 severe weather environments on a given day to identify the days with very large spatial coverage. **Figure 3.3a** shows the number of days each year with severe weather environments > 40 in the US associated with each peril. Similar to the nationally-aggregated counts of severe weather environments, there are large inter-annual fluctuations in the number of severe weather environments. There also appears to be a general decrease in the number of days with widespread severe weather environments. The decreasing trend in the 1990-2010 period is statistically significant with $p < 0.02$ for hail and wind, and $p < 0.15$ for tornado.

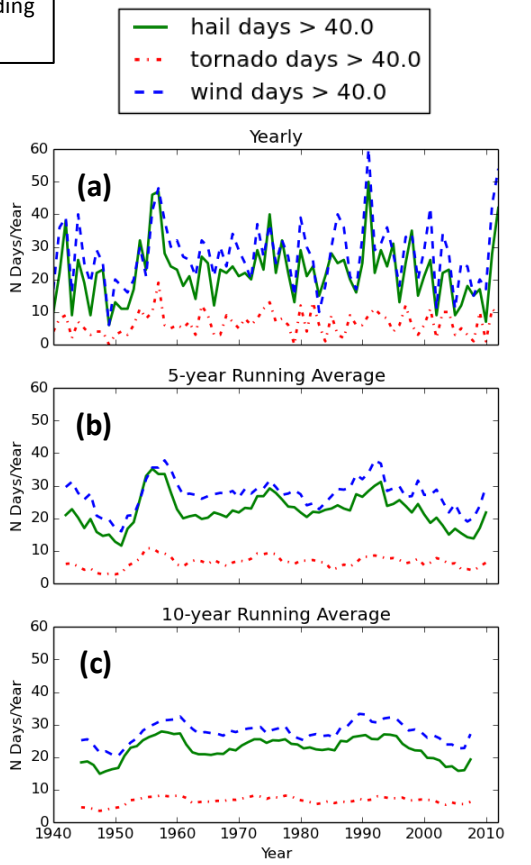

FIG. 3.3. (a) Number of days per year with widespread hail/tornado/wind environments (> 40) in the contiguous US. (b, c) 5- and 10-year running averages of (a).

3.1.2 US Regional Trends

Severe weather environments across the entire contiguous US have been on a fairly flat trend with relatively consistent totals relative to the long-term mean. However, the different regions of the US (**Fig. 2.2b**) exhibit considerably different behavior in trends and variance. **Figures 3.4** - **3.5** present the total annual hail environments (**Fig. 3.4**) and their 5-year running means and standard deviations within each of the five US regions (10-year running means of hail environments by region are shown in the Appendix A (**Fig. A.2**). All regions show considerable inter-annual variability in the total number of hail environments (**Fig. 3.4**). The West region shows small variability in hail environments before the 1970s which then changed to a regime of years of very high counts (e.g., 1982, 2004) interspersed with years of relatively less activity (e.g., 1990). However, as the West is the region with the fewest verified severe weather events for our MDD

training, confidence is low in these results. By contrast, the Plains and High Plains regions show a fairly consistent overall number of environments through the record with only a slight dip in the late 1940s for the Plains (**Fig. 3.4c**).

No statistically-significant trends are found for the Plains or the High Plains. The High Plains region displays short periods of relatively high activity and hence high variance in the late 1970s and again in the mid-2000s (**Fig. 3.5b**). The variance in the Plains region, however, is fairly consistent and somewhat high since the 1960s (**Fig. 3.5**). For the Plains, the standard deviation for 2003—2012 is not significantly different from any other high-variance 10-year period since 1940. The 2008—2012 standard deviation (262 env) is significantly (p < 0.2 per the F-test) different from variability in the late 1950s, however. For the High Plains, the 2008—2012 and 2003—2012 standard deviations are not significantly different from other periods of high variance (i.e., the 1970s).

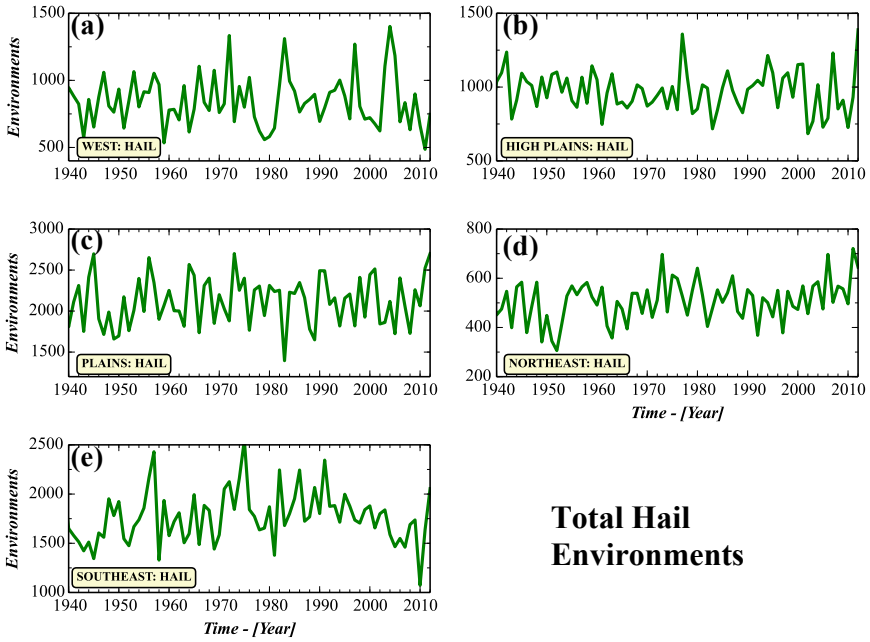

FIG. 3.4. The annual number of hail environments from 1940 – 2012 in the five US regions: (a) West, (b) Western High Plains, (c) Plains, (d) Northeast, and (e) Southeast.

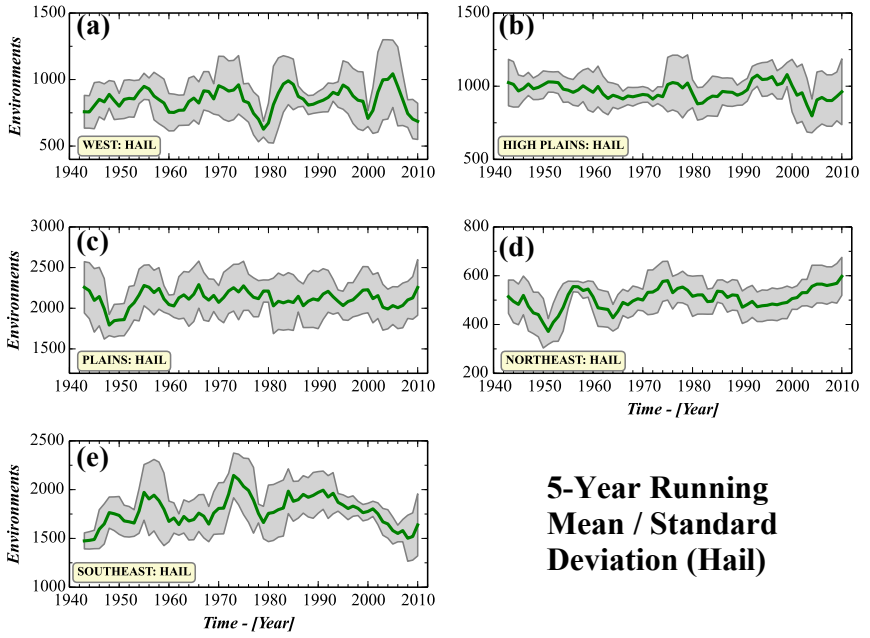

FIG. 3.5. 5-year running means of annual hail environments from 1940—2012 for the five US regions: (a) West, (b) Western High Plains, (c) Plains, (d) Northeast, and (e) Southeast. Gray shading represents ±1 standard deviation (5-year running) of the hail environments.

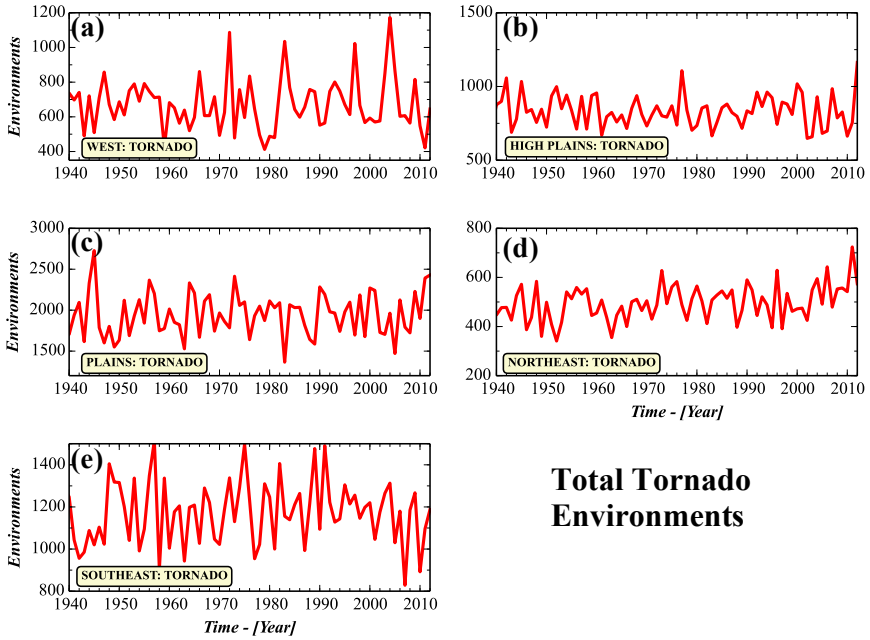

FIG. 3.6. As in **Fig. 3.4** but for tornado environments.

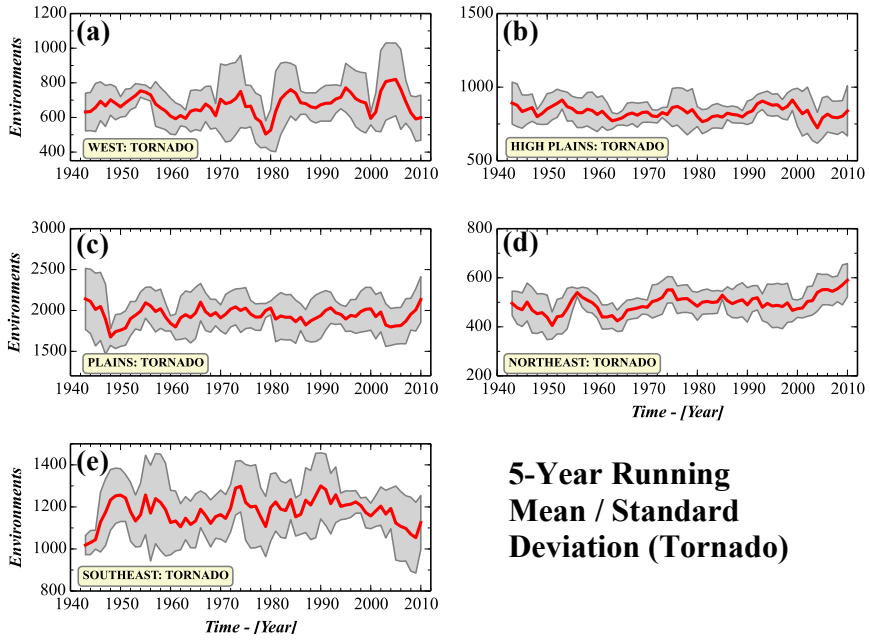

FIG. 3.7. As in **Fig. 3.5** but for tornado environments.

The changes in hail environments in the Northeast and the Southeast regions, however, illustrate significant changes, particularly in the latter part of the record. For the Northeast, a statistically-significant, *increasing* 20-year trend in hail-supportive environments exists (trend = 84.5 env./decade, $p < 0.05$). By contrast, a statistically-significant *decreasing* trend in hail environments is detected for the Southeast from the late 1980s through the 2000s (e.g., from 1991—2010 trend = -316 env./decade, $p < 0.01$). The 2008—2012 and 2003—2012 standard deviations in the Northeast and SouthEast are not significantly different from other high variance periods (e.g., the 1940s and the 1970s for the Northeast; the 1950s and 1960s for the Southeast).

For tornado environments (**Figs. 3.6 - 3.7**), similar regional trends and changes in variance are seen for the West, the Plains, and the High Plains in the raw and 5-year running-mean tornado environment counts. No statistically significant trends are observed in those regions. In terms of the high variance at the end of the record for those regions, this variance is not statistically different from other periods of similarly high variance since 1940. Elsewhere, an uptick (downtick) in tornado environments is visible for the Northeast (Southeast) from the late 1990s and into the 2000s. However, only the 10-year (1999–2008; trend = 118 env./decade) and 20-year (1992–2011; trend = 74 env./decade) trends in the Northeast are statistically-significant ($p < 0.05$) per the Mann-Kendall test. The 2008—2012 and 2003—2012 standard deviations in tornado environments in the Northeast and Southeast are not significantly different than other high-variance periods.

Finally, for the wind environments (**Fig. 3.8** and **Fig. 3.9**), no significant 10-, 15-, or 20-year are apparent for any region except the Southeast. There, a significant decreasing trend in total wind environments is detected from the early 1990s through the 2000s (e.g., the 1991—2010 trend = -242 wind env./decade, $p < 0.05$). In terms of interannual variability, the Plains region is the only region which experiences consistently high variability throughout the record (**Fig. 3.8**; middle left) and hence recent variability is not significantly higher than other periods. For all other regions, a recent increase in standard deviation for both 5-year and 10-year (**Fig. A.X**) periods is apparent but is insignificantly different from previous periods of relatively high variance (e.g., the 1970s in the High Plains and the late 1950s in the Southeast.

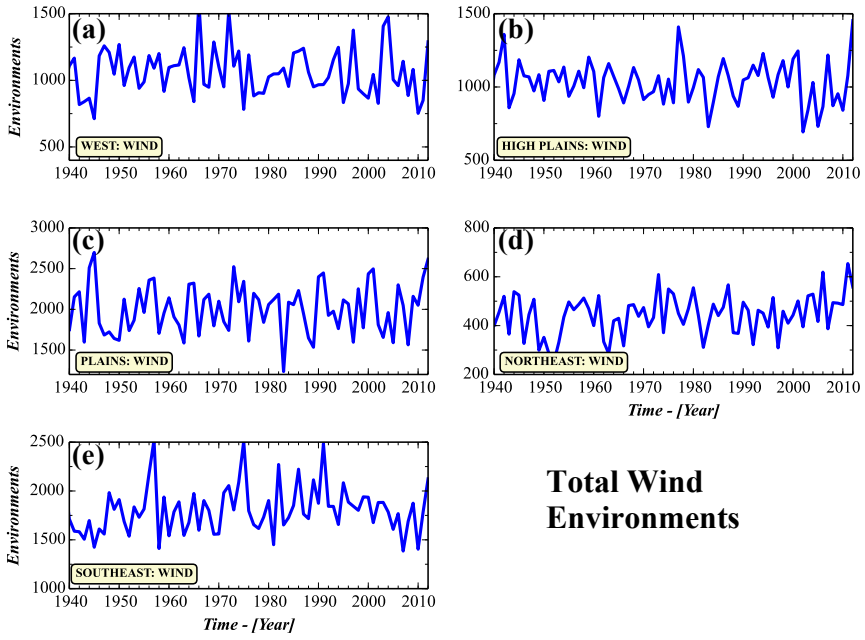

FIG. 3.8. As in **Fig. 3.4** but for wind environments.

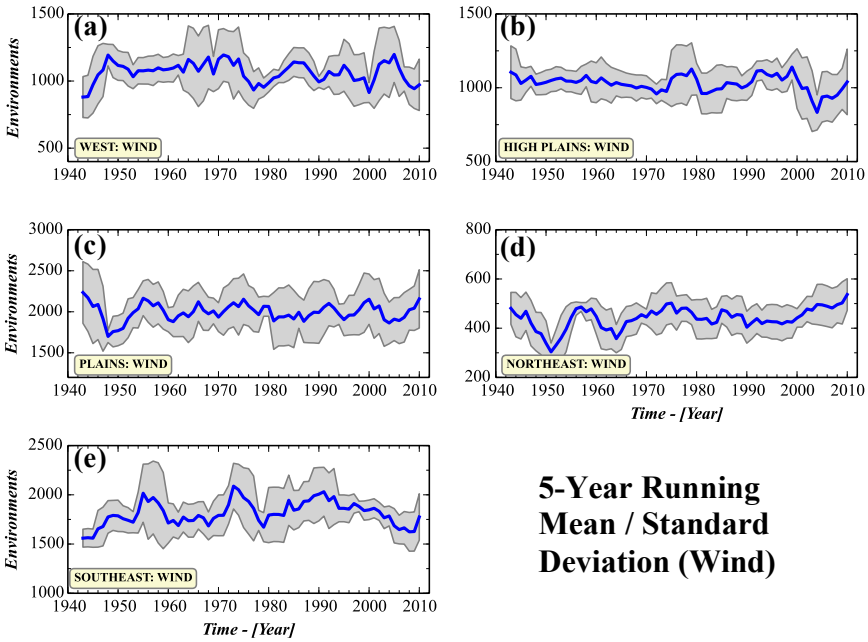

FIG. 3.8. As in **Fig. 3.5** but for wind environments.

Similar to **Figure 3.3**, we can consider the number of days per year with hail/tornado/wind environments covering greater than 50% of the Southeast and Northeast regions (> 17 and > 10 environments) where we observe trends of decreasing and increasing total number of severe weather environments in the last 20 years. **Figure 3.9a,b** show the number of days with environments exceeding this 50% threshold in the Southeast and Northeast regions (Figures for other regions do not exhibit any interesting trends, and are shown in the appendix, **A.X**). Similar to **Figure 3.3**, there are large inter-annual fluctuations in the yearly averages for all perils. More notably, the 5- and 10-year running averages show trends of increasing (decreasing) environments/day for the Northeast (Southeast) regions in the last 15-20 years.

In the Northeast, we observe statistically significant 20-year trends in of increasing average environments/day for hail, tornado, as well as wind ($p < 0.05$, $p < 0.05$, and $p < 0.1$ respectively) for the 1991-2011 period. This suggests that, not only is the number of severe weather environments increasing

for hail and tornado (**Figures 3.4d, 3.6d**), the extent of the severe weather environments on a given day is also increasing. In the Southeast, consistent with **Figures 3.4e and 3.8e**, we observe statistically significant 20-year trends of decreasing average environments/day for hail and wind ($p < 0.04$ and $p < 0.12$, respectively), and no trend of significance for tornado for the 1982-2010 period.

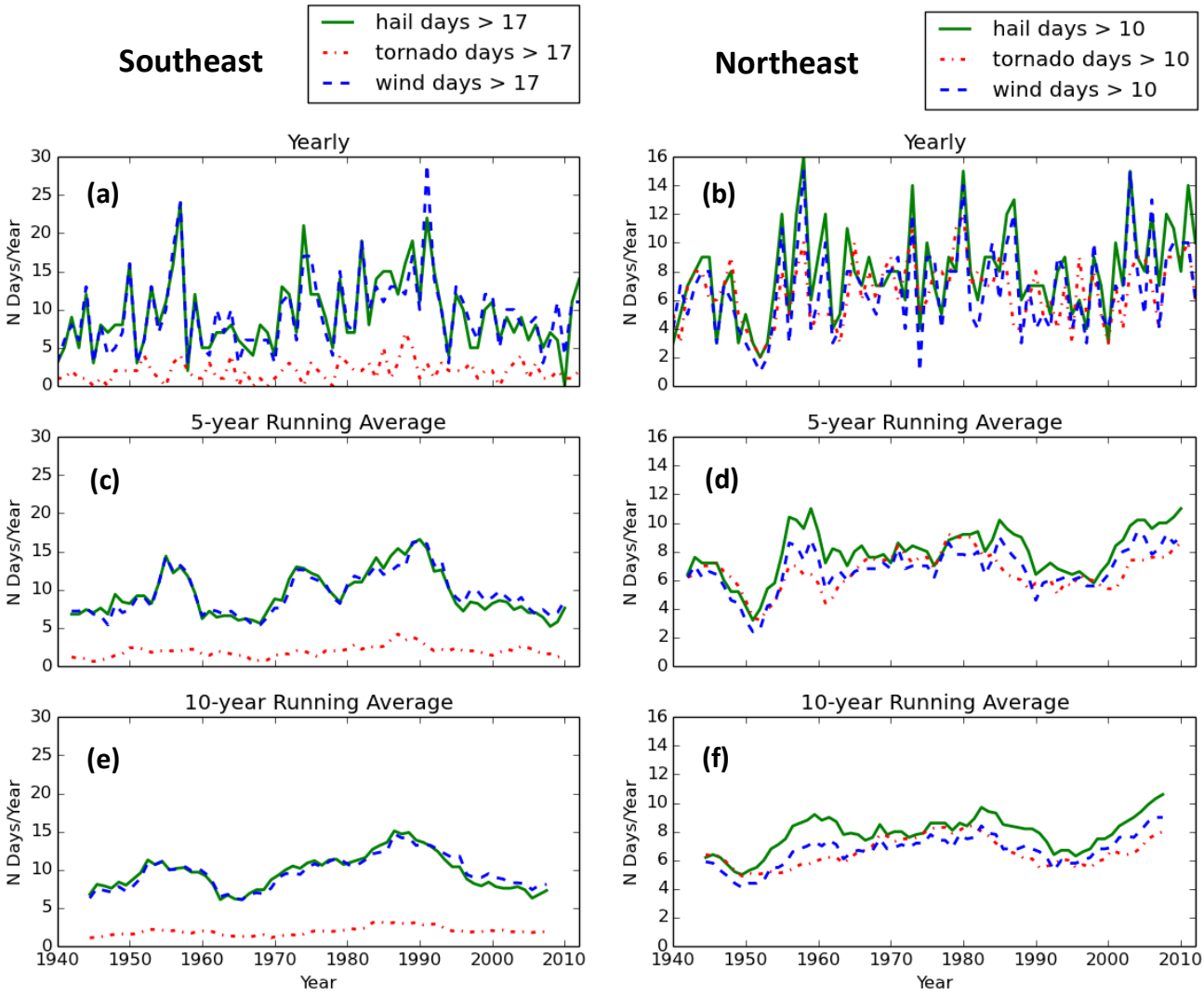

FIG. 3.9. (a, b) Number of days per year with hail/tornado/wind environments covering > 50% of the Southeast/Northeast regions (>17 and 10 environments, respectively). (c, d) 5-year running average. (e, f) 10-year running average.

3.1.3. Decadal Difference Maps

With annual counts examined annually for all regions, we now examine spatial changes in the mean hail, tornado, and wind environments during consecutive 10-year periods and see how the means have varied over the last 40+ years. **Figure 3.10** shows differences (expressed as percent changes in environments over the previous period) in 10-year mean hail environments between two consecutive 10-year periods covering the 1960s through the 2000s. Significance of the difference in the means

between the two periods is tested using a the *t*-statistic, and regions with 80% significance (dashed black contours) and 90% significance (solid black contours) are indicated in this and all subsequent mean difference plots. Because of the poor performance of the MMD in the West, we discount the large percent changes in that region for all environments. These spatial maps support our previous finding of a reduction of mean hail environments across the Southeast (~5-10% change in the mean between the 1990s and the 2000s), as shown in both **Figs. 3.10c** and **Fig. 3.10d**. Elsewhere, percent changes in mean hail environments change sign and magnitude as we compare from one decadal period to the next. For example, parts of the Northeast experienced significantly ($p < 0.2$; dashed black contour) higher mean hail environments during 1973—1982 compared to 1963—1972 (**Fig 3.10a**), but the following period (1982—1993) saw a significant *decrease* in mean hail environments compared to the prior ten years (**Fig. 3.10b**). This change in behavior from one epoch to the next is important to consider for these percent change maps – i.e., there is *no systematic change in the mean hail environments over much of the Lower 48 except possibly along the Gulf Coast and parts of the Southeastern US*.

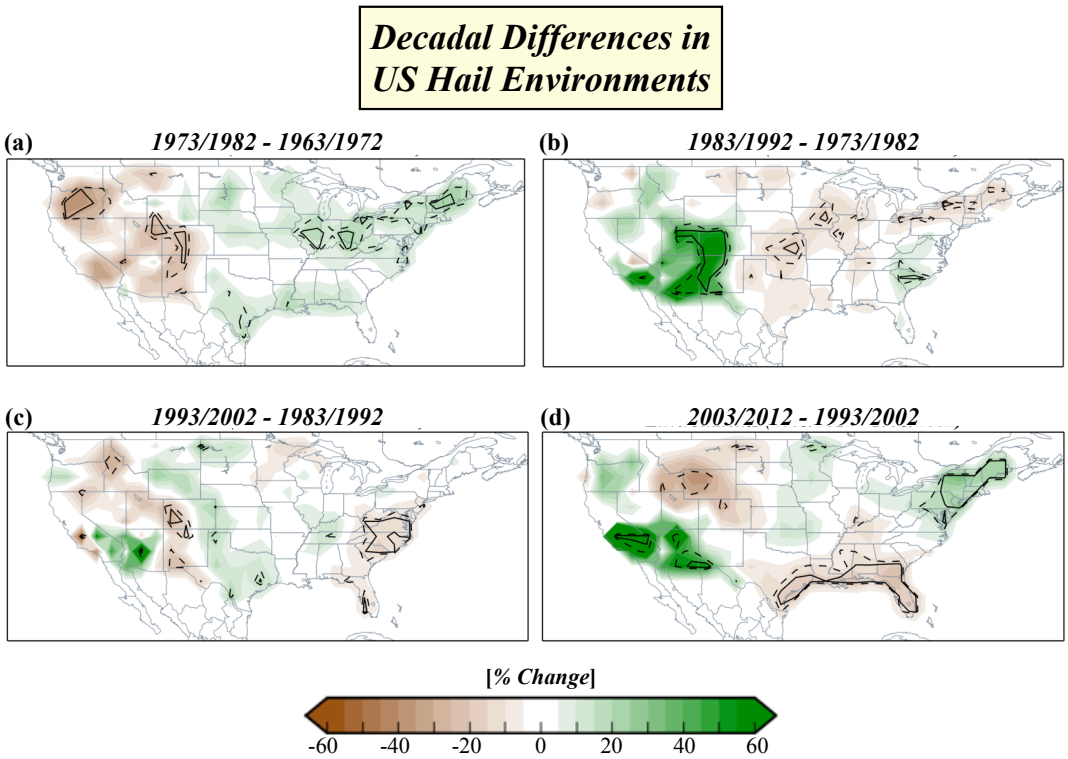

FIG. 3.10. The difference in the mean US hail environments between two consecutive 10-year periods (expressed as percent change from the previous period): (a) 1973 to 1982 minus 1963 to 1972, (b) 1983 to 1992 minus 1973 to 1982, (c) 1993 to 2002 minus 1983 to 1992, and (d) 2003 to 2012 minus 1993 to 2002. Dashed (solid) black lines denote the 80% (90%) significance levels for the difference in the two period means as tested by a two-tailed Student *t* test.

For tornado environments, **Figure 3.11** shows the percent changes in the mean number of environments between decadal periods for tornado environments. These changes in decadal means from one period to the next are also nonmonotonic across all regions, *indicating no systematic changes in the mean from the late twentieth century to present*. For the most recent period (2003—2012), there has been a significant difference (increase) in the mean number of tornado environments for the Northeastern US

over the 1993—2002 mean, but not significant trend in the number of tornado environments (**Fig. 3.6**). Finally, the mean number of wind environments per decade also does not show a systematic change over the 5 periods examined (**Fig. 3.12**), though 2003—2012 did have a significant ($p < 0.1$) increase (decrease) in the decadal-mean wind environments from the 1993—2002 period mean in the Northeastern US (Georgia and Florida) regions.

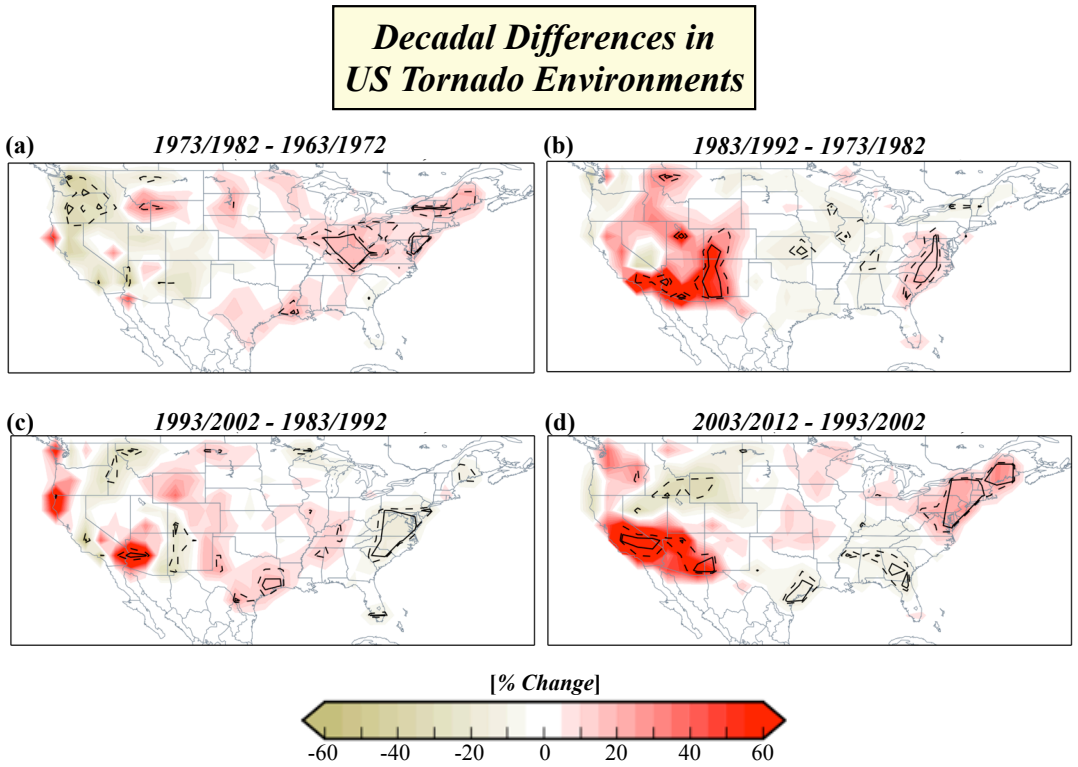

FIG. 3.11. As in **Fig. 3.10** but for changes in tornado environments.

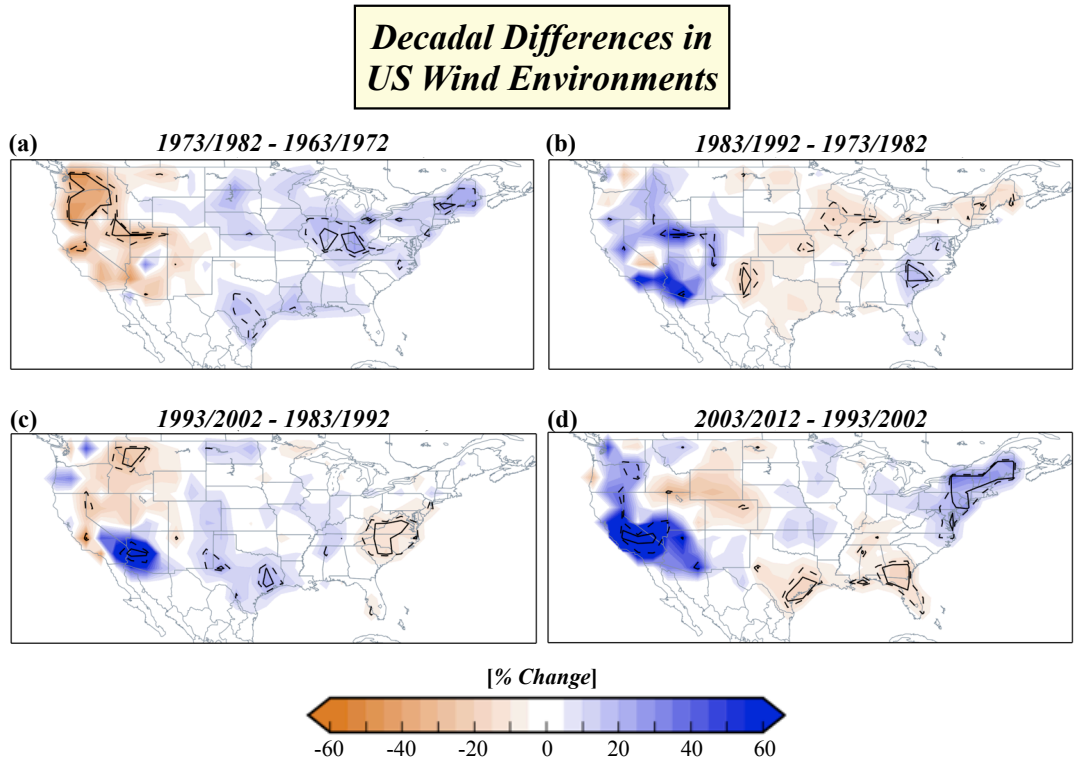

FIG. 3.12. As in **Fig. 3.10** except for changes in wind environments.

3.2 Canada

3.2.1 Overall Trends

The annual number of severe weather environments over Canada for the 1940-2012 period is shown in **Figure 3.13.** From 1940 – 1960, the overall number of severe weather environments remained fairly constant for all perils. Then, from about the mid-1960s through the late 1980s, the annual number of environments for all perils experienced a statistically significant downward trend (hail trend ≈ -310 env./decade, wind trend ≈ -350 env./decade, and tornado trend ≈ -220 env./decade; all significant at the 99% level per the Mann-Kendall test). A dramatic reversal of the trend commenced around 1990, with rapid *increases* in the number of environments for all perils (hail trend ≈ 1190 env./decade, wind trend ≈ 1245 env./decade, and tornado trend ≈ 800 env./decade, all significant at the 99% level per the Mann-Kendall test). Indeed, according to the MMD, the early twenty-first century consists of annual counts of environments for all perils across Canada at unprecedented levels since 1940 (**Fig. 3.13**). Since 2000, these environment counts have leveled off, and no detectable trend is observed in any peril.

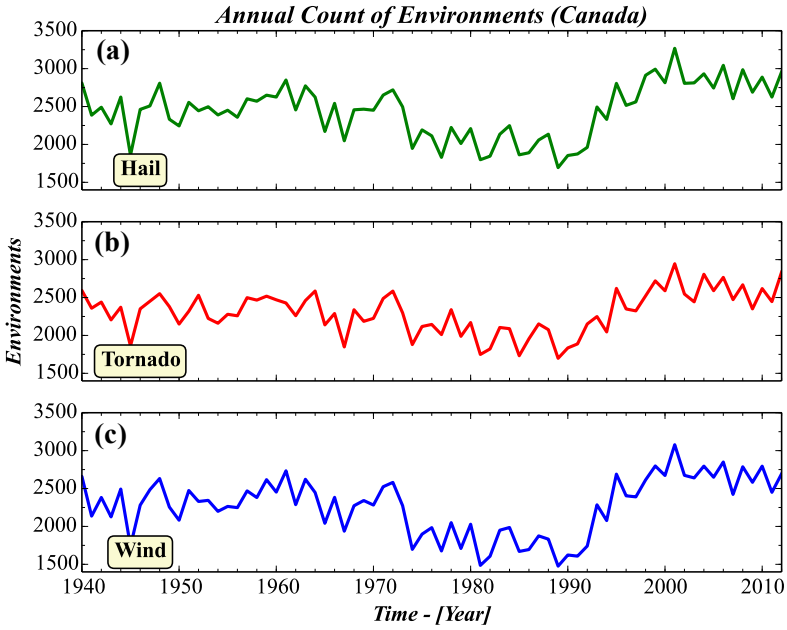

FIG. 3.13. The annual counts of (a) hail, (b) tornado, and (c) wind environments from 1940—2012 across Canada (see **Fig 2.2a**).

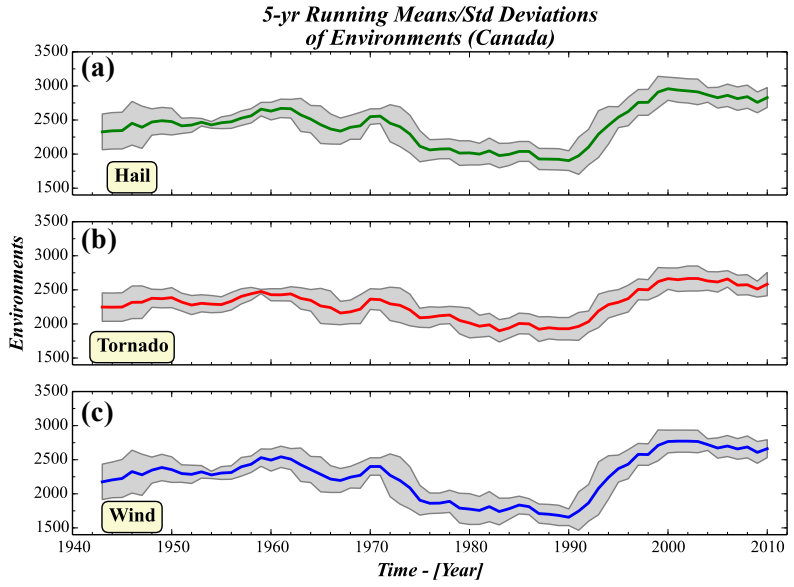

FIG. 3.14. 5-year running means of annual (a) hail, (b) tornado, and (c) wind environments from 1940—2012 across Canada Gray shading represents ±1 standard deviation (5-year running) of the environments.

To examine the variability in the annual severe weather environments in Canada, **Figure 3.14** presents the 5-year running mean and standard deviations of those environments. The downward trend from the mid-1960s into the 1980s and the rapid uptick in severe weather environments through the 1990s are very well apparent in all perils in both running means. In terms of variance, except for the 1940s, the 5-year running-standard deviation (gray shading; **Fig. 3.14**) is fairly consistent with a slight widening of the variance envelope in the late 1960s and early 1970s. The 2008—2012 and 2003—2012 standard deviation for all perils are not distinguishably higher than other periods since 1940 per the *F*-test. Decadal-mean and standard

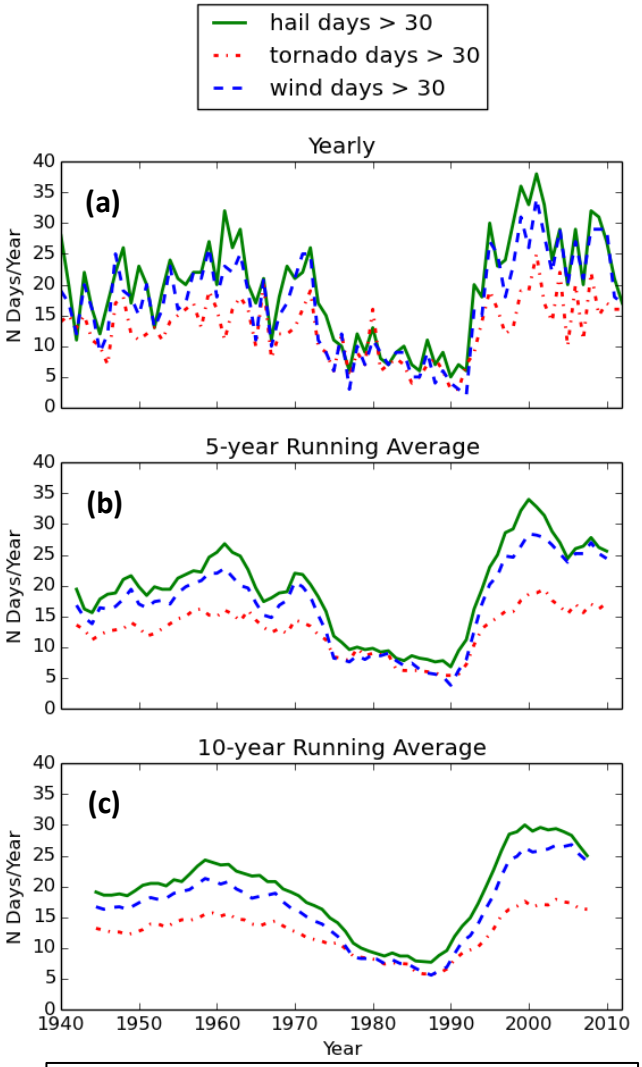

FIG. 3.15. (a) Number of days per year where the number of hail/tornado/wind environments was greater than 30. (b, c) 5- and 10-year running averages of (a).

deviations of the environment display similar trends for the 5-year running means and standard deviations (see **Appendix Figure A.X**).

As with the US, we also consider trends in the number days per year with widespread severe weather environments. Over the 73-year record period, the average number of severe weather environments per day in Canada is ~7. We choose a threshold of 30 severe weather environments on a given day to identify the days with very large spatial coverage. **Figure 3.15a** shows the number of days each year with > 30 severe weather environments in Canada associated with each peril, while **Figure 3.15b,c** show the 5- and 10-year running mean of the number of days exceeding our threshold.

Overall, the profile of the number of days with widespread severe weather environments follows the total number of severe weather environments very well – there is a large drop in both from the mid-1960s to the 1980s, followed by a large increase from the mid-1980s to 2000s. The 20-year increasing trend in between the 1981-2010 period is statistically significant to the 98% level ($p < 0.02$) for all perils. This suggests that, during this period, not only is the total number of severe weather environments increasing for all perils in Canada, but the number of days with a large number of severe weather environments is increasing as well, as opposed to having more days with an average number of severe weather environments.

3.2.2 Canadian Regional Trends

The broadscale features of the Canadian-wide annual environment counts vary somewhat as we analyze the four Canadian regions used in the MMD (**Fig. 2a**). For hail environments by region (**Fig. 3.16**), we find the rapid increase seen through the 1990s in ubiquitous in all regions except for British Columbia, where there is only a slight (but still significant at the 95% level) increasing trend from 1984/1985 to the mid-1990s. *Thus, the rapid increase in the number of hail environments seen in the 1990s is a nationwide phenomenon except for westernmost Canada*. In British Columbia, instead of a large upward trend since 1990, there is instead higher interannual variability in hail environments for that region. Prior to the ramp up, 20-year declining trends from mid-1960s to relative minima in the 1980s is significant ($p < 0.05$) in all regions except the Eastern Prairies. Finally, no statistically-detectable trend is apparent in any region since 2000 for the raw counts, similar to the findings over all of Canada (**Fig. 3.16**). However, in the 5-year running means (**Fig. 3.17**), there is a sizable downtick in hail environments over the Eastern Prairies. In accounting for the reduced degrees of freedom for the 5-year means, this trend is not

statistically significant. In regards to changes in the variability of the environments (**Fig. 3.15**), both the 2008—2012 and 2003—2012 standard deviations (**Fig. A.X**) are not significantly different or higher from any other 5- or 10-year period since 1940 in any region, as indicated via an *F*-test.

For the tornado environments in the Canadian regions (**Figs. 3.18** and **3.19**), the negative trend from the 1970s into the early 1980s is only statistically different from zero in the Eastern Canada and Maritimes region (**Fig. 3.18d**). More importantly, the strongly *positive* trend in tornado environments during the 1990s *is detectable in all regions for 20-year trends starting in the early 1980s* ($p < 0.01$), *but* is *only detectable in 10-year trends for the Western and Eastern Prairies* ($p < 0.05$) per the Mann-Kendall test. Hence, for example, the point of most rapid uptick in tornado environments seen for Eastern Canada and the Maritimes (**Fig. 3.18d**) is also a period of high variability for tornado environments (**Figs. 3.19d** and **A.X**) and thus precludes assigning any significance to the shorter 10-year trend. In terms of changes in the variance, no region exhibits recent variability that is significantly different from the late from any other 5- or 10-year period since 1940.

Finally, the annual number of wind environments over the Canadian regions (**Fig. 3.20**) shows a statistically significant ($p < 0.05$) upward trend during from the late

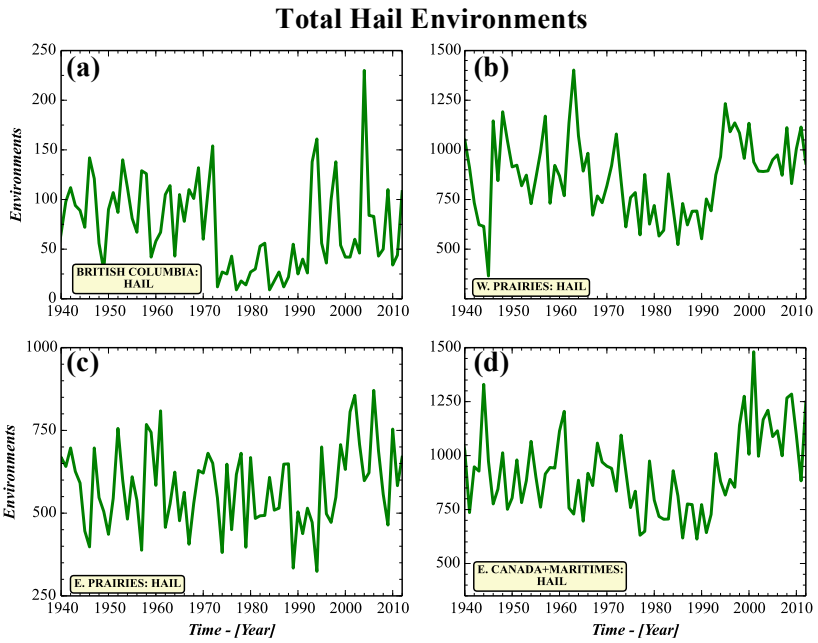

FIG. 3.16. The annual number of hail environments from 1940 – 2012 in each of the four Canadian regions: (a) British Columbia, (b) Western Prairies, (c) Eastern Prairies, and (d) Eastern Canada and the Maritimes.

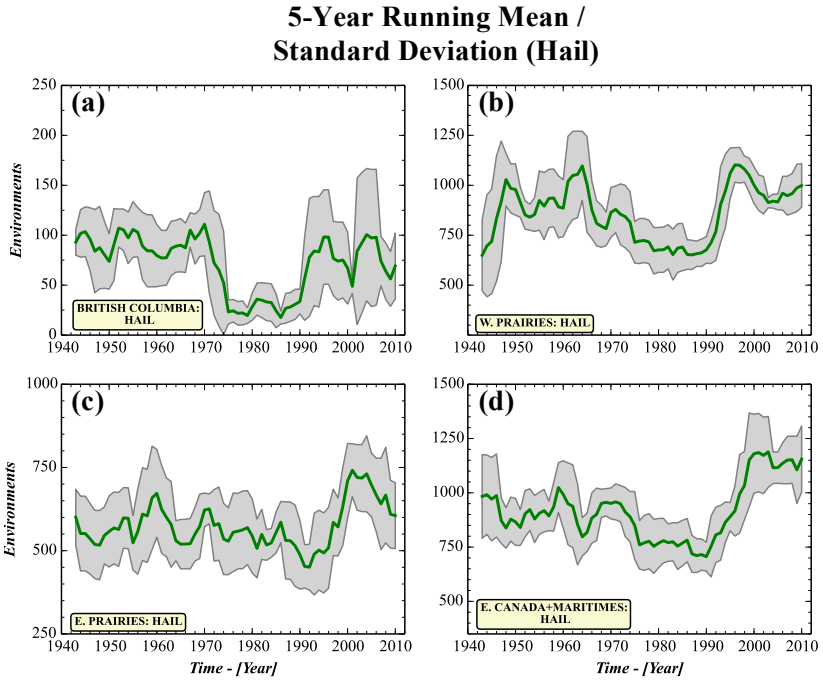

FIG. 3.17. 5-year running means of annual hail environments from 1940—2012 in each of the Canadian regions: (a) British Columbia, (b) Western Prairies, (c) Eastern Prairies, and (d) Eastern Canada and the Maritimes. Gray shading represents ±1 standard deviation (5-year running) of the hail environments.

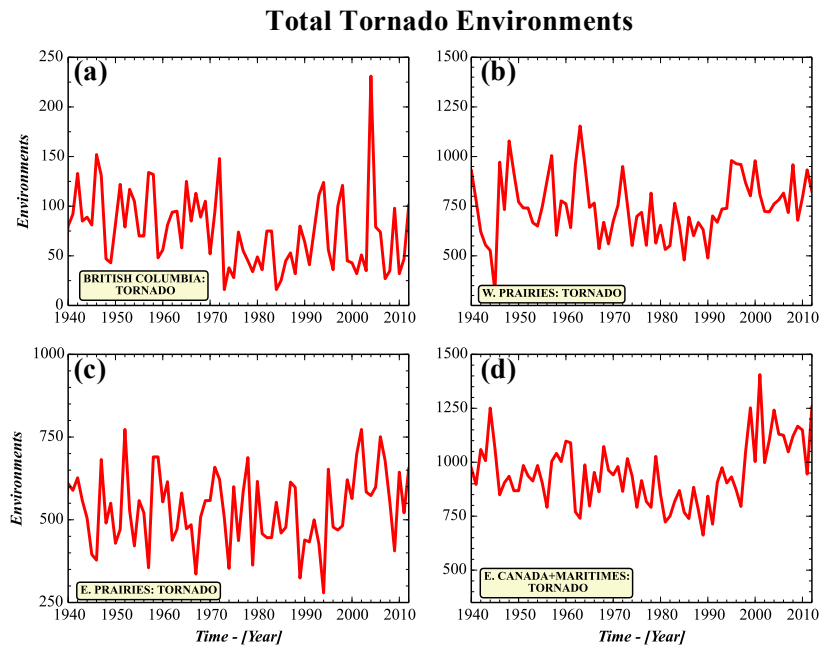

FIG. 3.18. As in **Fig. 3.16** but for tornado environments.

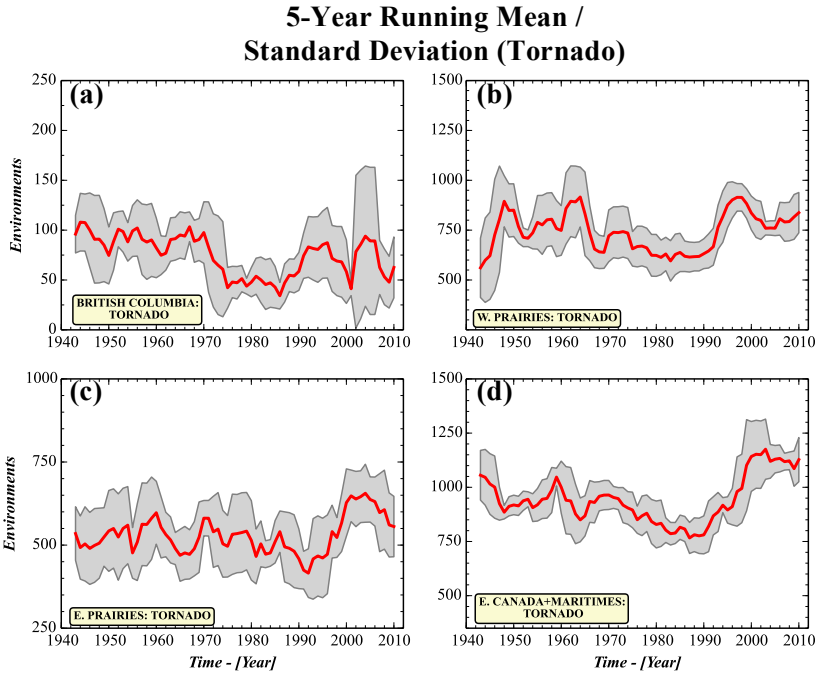

FIG. 3.19. As in **Fig. 3.17** but for tornado environments.

1980s through the 1990s in all regions except for British Columbia. This period of increasing wind environments follows a period of lower environments in the late 1970s and 1980s, but only Eastern Canada and the Maritimes and the Western Prairies experienced a statistically significant negative trend from the early 1970s into the mid-1980s ($p < 0.05$). Both the 2008—2012 (**Fig. 3.21**) and 2003—2012 standard deviations (**Fig. A.X**) in the wind environments are indistinguishable from other 5- and 10-year periods in the recent past across all regions, indicating no systematic change in the interannual or decadal variability of wind environments in Canada.

Finally, we consider how the number of days per year with a large number of severe weather environments breaks down regionally. Recall that for the overall trend in Canada exhibited a statistically significant increase in the number of days with a large number of severe weather environments in the last 30 years (**Figure 3.15**). When we break this down regionally, the trend appears to hold, although the periods of this increasing trend manifests itself differently in each region. **Figures 3.22a,b & 3.23a,b** show the number of days with environments exceeding 33% of the area in each of the four regions. The lowered threshold compared to the 50% used for the Northeast and Southeast regions in the US is due to the fact that widespread severe weather environments appear to be much less common, and a 50% threshold results in very few days per year (0-2) exceeding it.

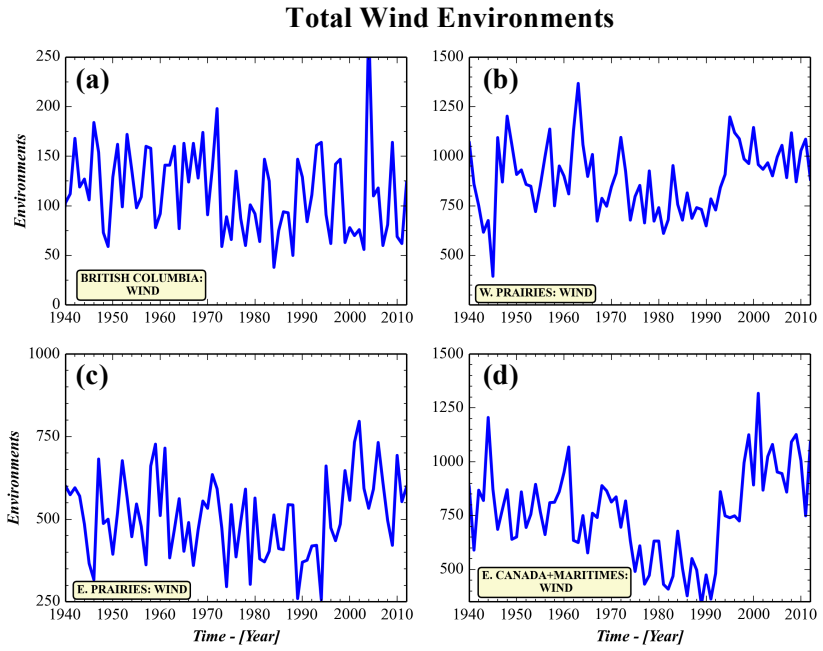

FIG. 3.20. As in **Fig. 3.16** but for wind environments.

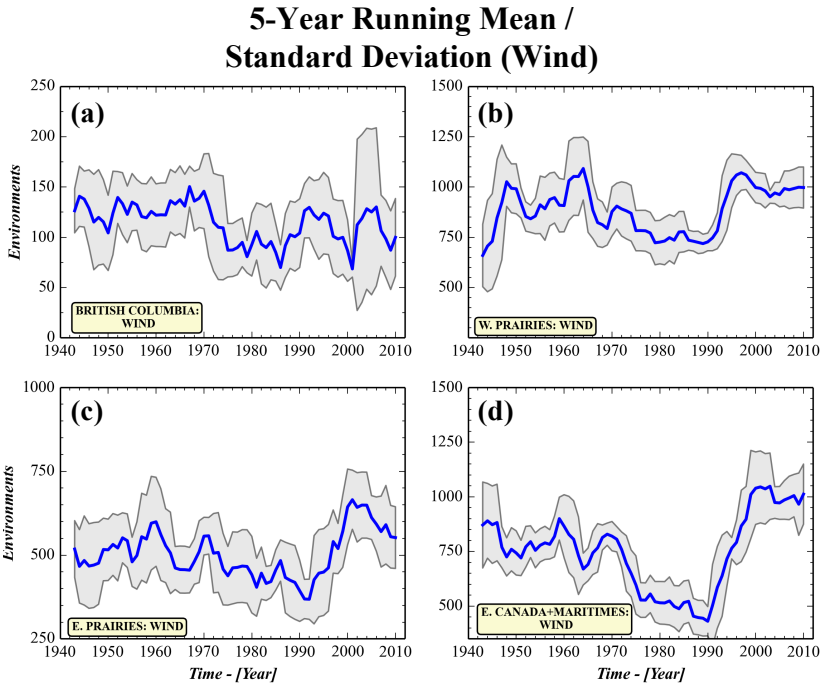

FIG. 3.21. As in **Fig. 3.17** but for wind environments.

British Columbia region **(Figure 3.22a,c,e)** – only hail environments show a statistically significant increasing trend ($p < 0.1$) from 1984-2008. This is most likely due to the weakness of the West MMD model from the lack of SPC reports to train against. In the Western Prairies, there is an increasing trend of days per year with a large number of severe weather environments for all between the 1980s to the mid-2000s for all three perils (**Figure 3.22b,d,f**, $p < 0.02$, 0.05, 0.07 for hail, tornado, and wind, respectively). Notably, there is a pronounced increase in the trend between 1990 and 1995 that appears to be steeper than the rest of the regions.

In the Eastern Prairies, we also observe an increasing trend, although the period starts later than the other regions, from 1988 to 2008 for all three perils (**Figure 3.23a,c,e**, $p < 0.03$, 0.04, and 0.1 for hail, tornado, and wind). Finally, the most gradual upward trends are observed in the Eastern Canada & Maritimes region (**Figure 3.23b,d,f**) from 1977-2009 ($p < 0.1$, 0.08, and 0.02 for hail, tornado, and wind).

3.2.3 Decadal Difference Maps

With nationwide and regional trends in total annual severe weather environments, we now examine differences in decadal-means of these environments to search for potential changes. **Figure 3.24** shows this difference for hail environments across Canada. Focusing on the changes in the latest decade (2003—2012; **Fig. 3.24d**), we see that there is a significant increase (~10-15%; $p < 0.2$) in the mean number of hail environments over the 1993—2002 decadal-mean for parts of eastern Ontario. A significant decline in mean hail environments from 1993—2002 to 2003--2012 is observed across much of northern Saskatchewan (-10% to -15%; $p < 0.2$). These

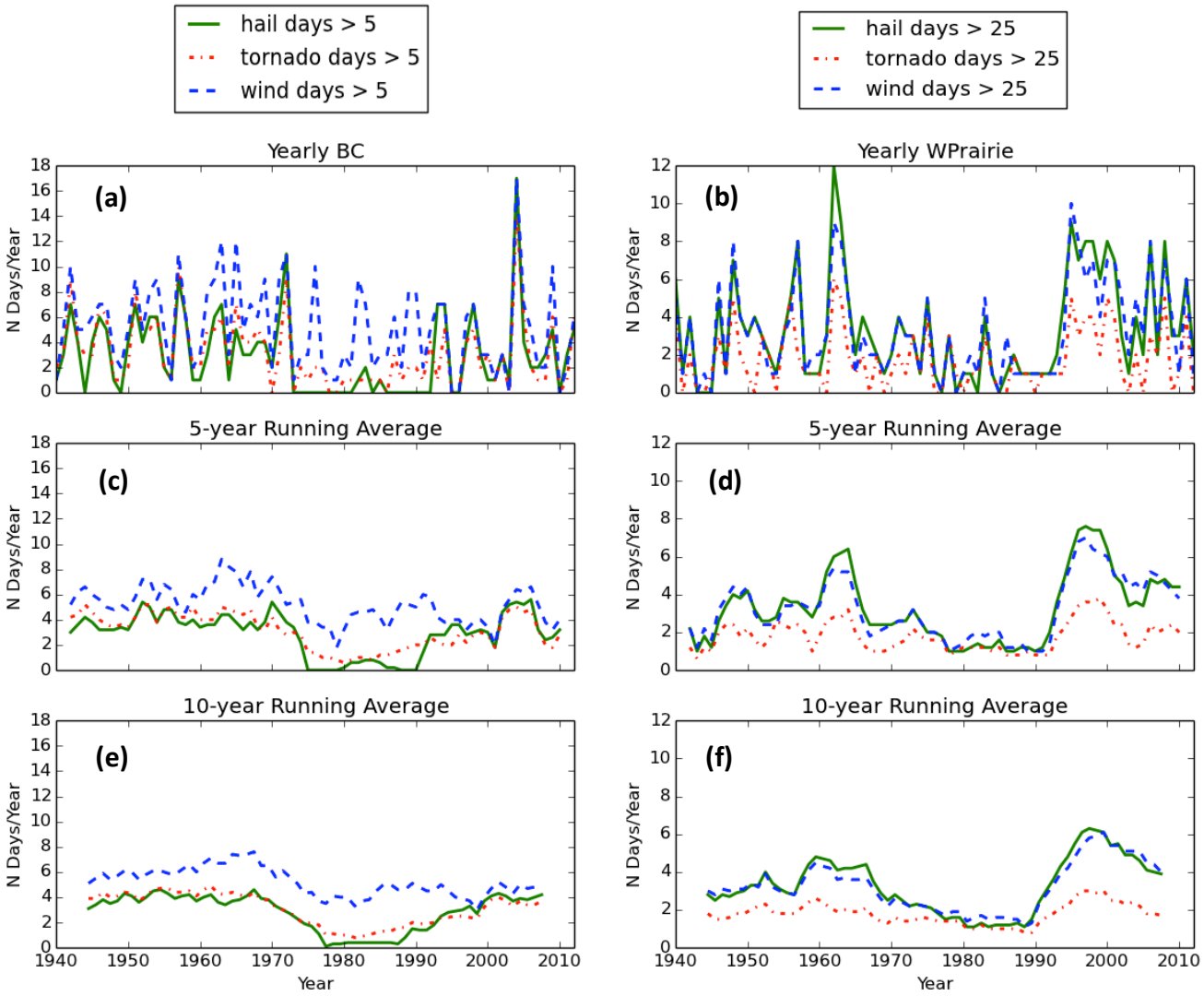

FIG. 3.22. (a, b) Number of days per year with hail/tornado/wind environments covering > 33% of the British Columbia/Western Prairies regions (>5 and 25 environments, respectively). (c, d) 5-year running average. (e, f) 10-year running average.

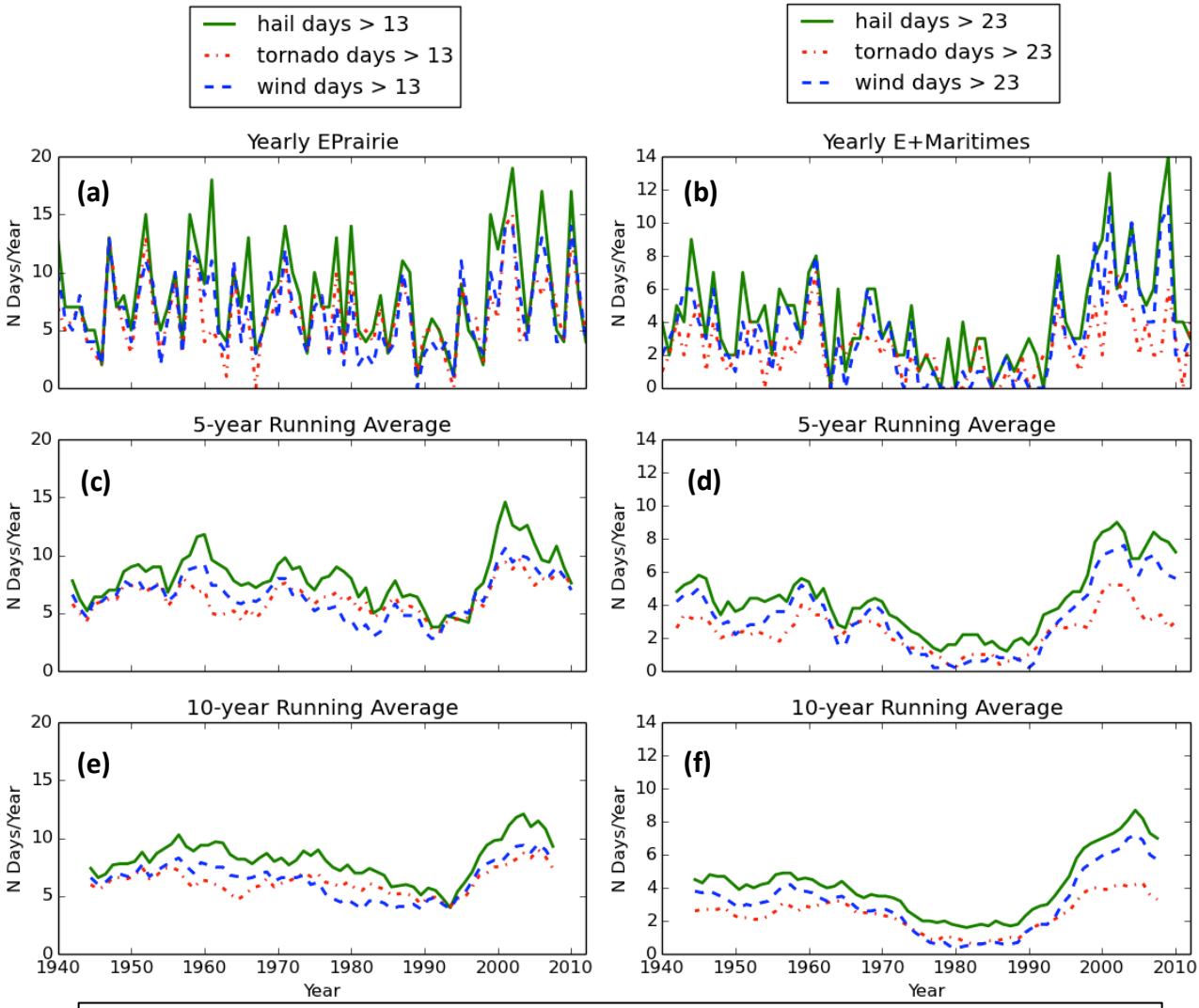

FIG. 3.23. (a, b) Number of days per year with hail/tornado/wind environments covering > 33% of the Eastern Prairies/Eastern Canada & Maritimes regions (> 13 and 23 environments, respectively). (c, d) 5-year running average. (e, f) 10-year running average.

differences in the mean, however, pale in comparison to extremely large (>60%) change in mean hail environments experienced between the 1983—1992 and 1993—2002 decadal periods (**Fig. 3.24c**). The change seen here immediately reflects the unprecedented rise in the hail environments observed for all of Canada (**Figs. 3.13** and **3.14**) and regionally (**Figs. 3.16** and **3.17**). The large increase in the mean environments is ubiquitous across all of Canada *except for parts of British Columbia, eastern Manitoba, and most of Ontario* where the meandifferences are barely significant at the 80% level. This pattern of changes in decadal-means in **Fig. 3.24c** may be a reflection of our model implementation across the Eastern Prairies region (i.e., using the Plains model from the US). For the prior 3 decadal periods, we see quite different changes in the mean which large areas of significant *decreases* in means from the 1960s into the 1970s for the western half of Canada and parts of Quebec (**Fig. 3.24a**), but no significant changes are seen between the 1973—1982 and the 1983—2002 decadal means (**Fig. 3.24b**).

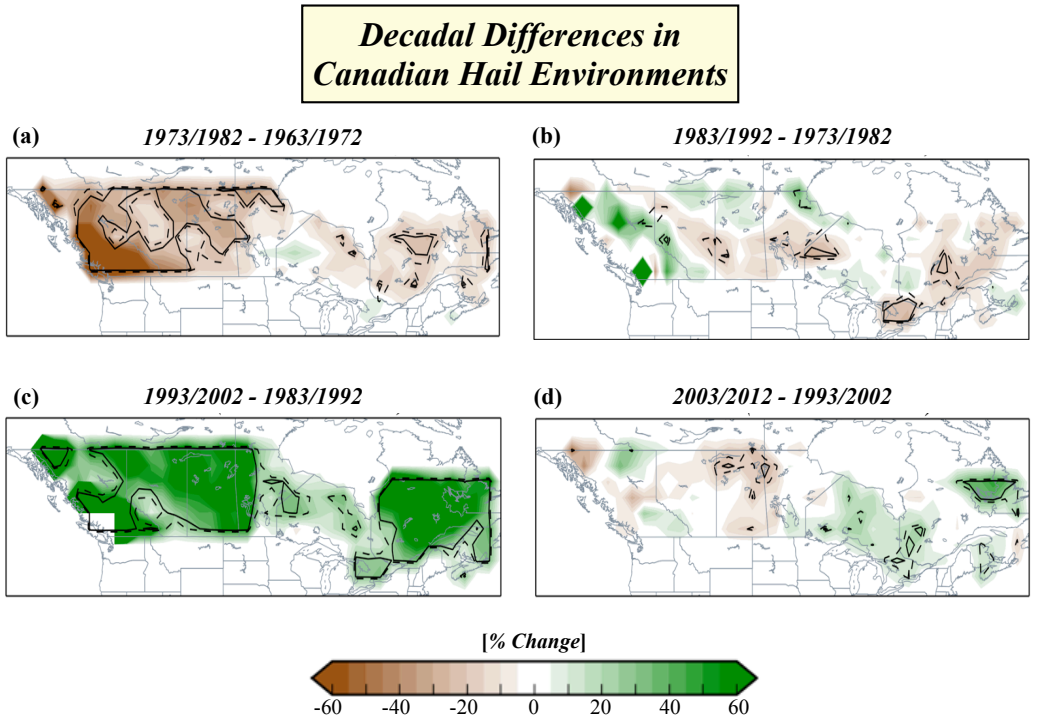

FIG. 3.24. The difference in the mean Canada hail environments between two consecutive 10-year periods (expressed as percent change from the previous period): (a) 1973 to 1982 minus 1963 to 1972, (b) 1983 to 1992 minus 1973 to 1982, (c) 1993 to 2002 minus 1983 to 1992, and (d) 2003 to 2012 minus 1993 to 2002. Dashed (solid) black lines denote the 80% (90%) significance levels for the difference in the two period means as tested by a two-tailed Student *t* test.

For changes in decadal-means in tornado environments (**Fig. 3.25**), the mean changes are of the same sign and spatially similar to the hail environments for the 1993—2002 and 1983—1992 (**Fig. 3.25c**) the 2003—2012 and 1993—2002 (**Fig. 3.25d**) period comparisons. For the former, note that the largest percent changes in the decadal means appear in northern Quebec and northern Manitoba and Saskatchewan, where incidence of these events is climatologically low (***reference some climo figure from literature?***), and the >60% change seen in British Columbia is likely spurious given model performance there (**Fig. 3.25c**). For earlier decadal-mean differences, we see a slightly different pattern, as the decrease in tornado environments from the 1960s into the 1970s was mainly confined to British Columbia and southern Alberta ($p < 0.1$; **Fig. 3.25a**). No significant difference in decadal means are seen throughout Canada from the 1970s into the 1980s (**Fig. 3.25b**).

Finally, the changes in decadal-means for the wind environments (**Fig. 3.26**) show a similar pattern to the hail and tornado environments for the most recent decadal differences (**Figs. 3.26c** and **3.26d**), except that the change in the mean experienced during 1993—2002 over 1983—1992 is also significantly different over much of Ontario (**Fig. 3.26c**). For the earlier periods, the decline in the mean wind environments from the 1960s to the 1970s was concentrated a lot in Eastern Canada and the Maritimes (**Fig.3.26a**), with percent changes in the mean of over -20% from the 1960s to the 1970s. In the 1970s to 1980s transition, some significant ($p < 0.2$) changes in wind environments are visible for Eastern Canada only.

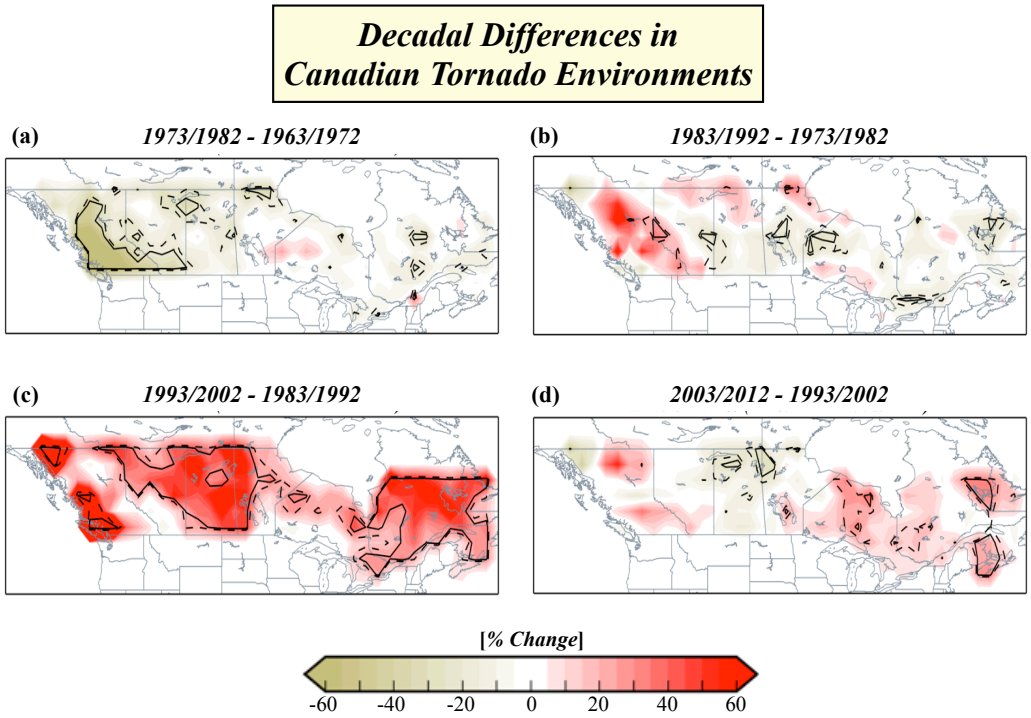

FIG. 3.25. As in **Fig. 3.24** but for tornado environments.

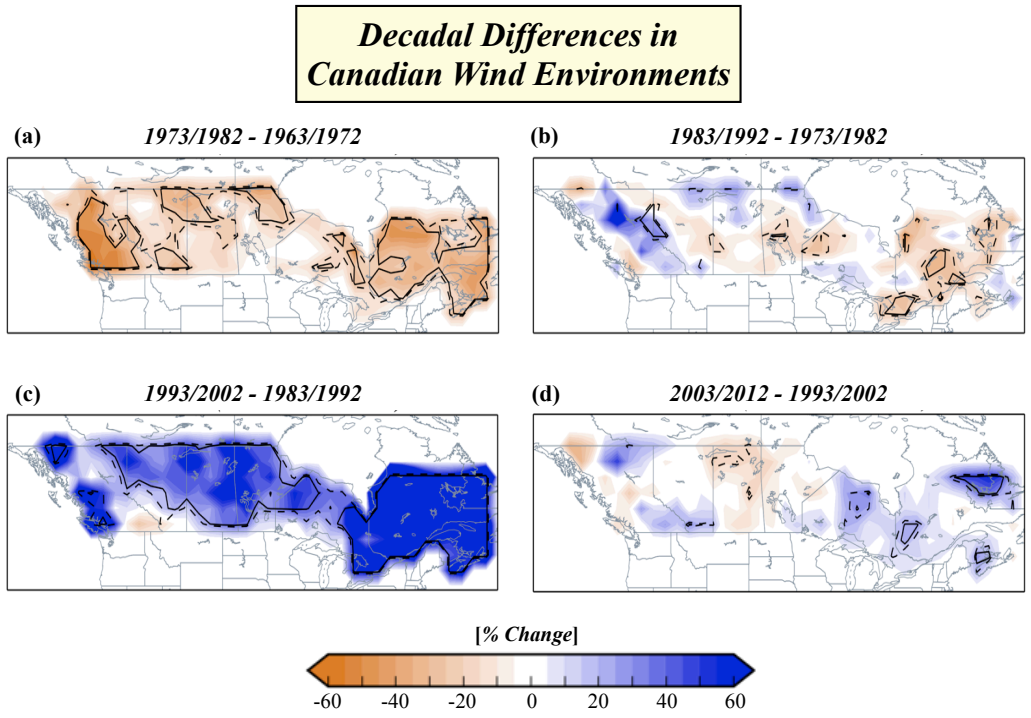

FIG. 3.26. As in **Fig. 3.24** but for wind environments.

References

Alexander, M. A., K. H. Kilbourne, and J. A. Nye, 2014: Climate variability during warm and cold phases of the Atlantic Multidecadal Oscillation (AMO) 1871–2008. *J. Marine Sys.*, **133**, 14 – 26.

Anderson, B. T., J. C. Furtado, K. M. Cobb, and E. Di Lorenzo, 2013: Extratropical forcing of El Niño–Southern Oscillation asymmetry. *Geophys. Res. Lett.*, **40**, 4916 – 4921.

Brooks, H. E., J. W. Lee, and J. P. Craven, 2003: The spatial distribution of severe thunderstorm and tornado environments from global reanalysis data. *Atmos. Res.*, **67-68**, 73-94.

Brooks, H. E., 2013: Severe thunderstorms and climate change. *Atmos. Res.*, **123**, 129-138.

Capotondi, A., 2013: ENSO diversity in the NCAR CCSM4 climate model, *J. Geophys. Res.*, **118**, 4755—4770.

Chang, V. Y., Arhonditsis, G. B., Sills, D. M., Auld, H., Shephard, M. W., Gough, W. A., and Klaassen, J., 2013: Probability of tornado occurrence across Canada. *J. Climate*, **26**, 9415—9428.

Compo, G. P., and Coauthors, 2011: The Twentieth Century Reanalysis Project. *Quart. J. Roy. Meteor. Soc.*, **137**, 1 – 28.

Cortes, C., and Vapnik, V., 1995: Support-vector networks. *Machine Learning*, **20**, 273—297.

Dee, D. P., and Coauthors, 2011: The ERA-Interim reanalysis: Configuration and performance of the data assimilation system. *Quart. J. Roy. Meteor. Soc.*, **137**, 553 – 597.

Doswell, C., Brooks, H., and Kay, M., 2005: Climatological estimates of daily local nontornadic severe thunderstorm probability for the United States. *Wea. Forecasting*, **20**, 577-595

Environment Canada, 1987: Climate Atlas of Canada, Map Series 3, Pressure, Humidity, Cloud, Visibility, and Days with Thunderstorms, Hail, Smoke, and Haze, Fog, Freezing Precipitation, Blowing Snow, Frost, Snow on the Ground*, Ministry of Supply and Services*, Cat. No. EN56-63/3-1986

Etkin, D., and Brun, S. K., 1999: A Note on Canada's Hail Climatology: 1977-1993. *Int. J. Climatol.*, **19**, 1357—1373.

Fujita, T., 1975: Super Outbreaks of Tornadoes of April 3-4, 1974. Map printed by the University of Chicago Press.

Gan, B., and L. Wu, 2013: Centennial trends in Northern Hemisphere winter storm tracks over the twentieth century, *Quart. J. Roy. Meteor. Soc.*, doi: 10.1002/qj.2263

Gensini, V. A., and W. S. Ashley, 2011: Climatology of potentially severe convective environments from North American Regional Reanalysis. *Electronic J. Severe Storms Meteor.*, **6**, 1 – 40.

Grünwald, S., and H. E. Brooks, 2011: Relationship between sounding derived parameters and the strength of tornadoes in Europe and the USA from reanalysis data. *Atmos. Res.* , **100**, 479—488.

Insurance Bureau of Canada, 2014: Facts of the Property and Casualty Insurance Industry. [Available online at: http://www.ibc.ca/en/Need_More_Info/Facts_Book/index.asp.]

Kalnay, E., and Coauthors, 1996: The NCEP/NCAR 40-year reanalysis project, *Bull. Amer. Meteor. Soc.*, **77**, 437 – 470.

Lee, C. C., 2012: Utilizing synoptic climatological methods to assess the impacts of climate change on future tornado-favorable environments. *Nat. Hazards*, **62**, 325-343.

Lock, N. A., and A. L. Houston, 2014: Empirical examination of the factors regulating thunderstorm initiation. *Mon. Wea. Rev.*, **142**, 240 – 258.

Marsh, P. T., H. E. Brooks, and D. J. Karoly, 2007: Assessment of the severe weather environment in North America simulated by a global climate model. *Atmos. Sci. Lett.*, **8**, 100-106.

Marsh, P. T., H. E. Brooks, and D. J. Karoly, 2009: Preliminary investigation into the severe thunderstorm Environment of Europe simulated by the Community Climate System Model 3. *Atmos. Res.,* **93**, 607 – 618.

Moore , G. W. K., I. A. Renfrew, and R. S. Pickart, 2013: Multidecadal mobility of the North Atlantic Oscillation. *J. Climate*, **26**, 2453 – 2466.

Munich Re, 2014: 2013 Natural Catastrophe Year in Review. [Available online at: http://www.munichreamerica.com/site/mram/get/documents_E1433556406/mram/assetpool.mr_america/PDFs/4_Events/MunichRe_III_NatCatWebinar_012014.pdf.]

Paruk, B. J., and S.R. Blackwell, 1994: A severe thunderstorm climatology for Alberta. *Nat. Wea. Digest,* **19**, 27-33

Robinson, E. D., R. J. Trapp, and M. E. Baldwin, 2013: The geospatial and temporal distributions of severe thunderstorms from high-resolution dynamical downscaling. *J. Appl. Meteor. Climatol.*, **52**, 2147 – 2161.

Smith, B. T., Thompson, R. L., Grams, J. S., and Broyles, C., 2012: Convective Modes for Significant Severe Thunderstorms in the Contiguous United States. Part 1: Storm Classification and Climatology. *Wea. Forecasting*, **27**, 1114-1135

Trapp, R. J., N. S. Diffenbaugh, H. E. Brooks, M. E. Baldwin, E. D. Robinson, and J. S. Pal, 2007: Changes in severe thunderstorm environment during the 21st century caused by anthropogenically enhanced global radiative forcing. *Proc. Natl. Acad. Sci. U. S. A.*, **104**, 19,719 – 19,723.

Trapp, R. J., N. S. Diffenbaugh, and A. Gluhovsky, 2009: Transient response of severe thunderstorm forcing to elevated greenhouse gas concentrations. *Geophys. Res. Lett.*, **36**, L01703, doi:10.1029/2008GL036203.

van Klooster, S.L., and P. J. Roebber, 2009: Surface-based convective potential in the contiguous United States in a business-as-usual future climate. *J. Climate*, **22**, 3317 – 3330.

Woollings, T., C. Czuchnicki, and C. Franzke, 2014: Twentieth century North Atlantic jet variability. *Quart. J. Roy. Meteor. Soc.*, **140**, 783 – 791.